Myrmecological News
ISSN 1997-3500
myrmecologicalnews.org
Myrmecol. News 35: 161-188 doi: 10.25849/myrmecol.news_035:161 19 June 2025
Original Article

The larval morphology of the clonal raider ant, *Ooceraea biroi* (Forel, 1907) (Dorylinae), with broader implications for the Formicidae and Hymenoptera

Di Li, Adrian Richter, Leonora Olivos-Cisneros, Thomas van de Kamp, Daniel J.C. Kronauer, Rolf G. Beutel & Brendon E. Boudinot

Abstract

The larvae of ants are essential for colony organization and growth, yet knowledge of their internal anatomy is sparse, and the homologies of many larval structures remain uncertain. We therefore used synchrotron-radiation micro-computed tomography (SR-µ-CT) and scanning electron microscopy (SEM) to investigate, respectively, the internal and external morphology of the larva of the clonal raider ant, *Ooceraea biroi* (Forel, 1907), a model species for experimental biology. The documented characters are compared with conditions found in other Formicidae and Hymenoptera, and more broadly with features of larvae of other orders of Holometabola. As in other groups of Aculeata (and Orussidae), the body of *Ooceraea* is grub-like and depigmented, with distinctly reduced cephalic structures, and a weakly sclerotized, strongly simplified, sausage-like postcephalic body. This larval pattern reflects a distinct simplification compared with immature stages in the symphytan grade, with completely reduced eyes, antennae, and extrinsic labral muscles, vestigial palps, and missing thoracic legs and abdominal prolegs. Despite a simplified and largely uniform body configuration in apocritan larvae, including ants, there is considerable variation. Larvae of Formicidae vary distinctly in external features, especially in the general body shape, setation, and mandibular teeth. We therefore summarize eight morphological characters from previous studies to contextualize our findings, highlighting the often-underestimated diversity of larval morphology, which provides fertile ground for future study. Our study extends the knowledge of the external and internal morphology of ant larvae by taking a multi-modal approach to phenotype sampling, particularly via µ-CT. These methods have the potential of rapidly increasing the knowledge of previously neglected larval morphology, facilitating deeper investigations of evolutionary transformations in immature stages and providing a more complete picture of the evolution of an ecologically paramount group of insects.

Key words: Phenomics, anatomy, Micro CT, 3D-reconstruction.

Received 3 July 2024; revision received 24 March 2025; accepted 10 April 2025
Subject Editor: Alexander S. Mikheyev

Di Li, College of Plant Protection, South China Agricultural University, 510642 Guangzhou, China; Friedrich-Schiller-Universität Jena, Institut für Zoologie und Evolutionsforschung, 07743 Jena, Germany; Senckenberg Research Institute and Natural History Museum, Senckenberganlage 25, 60325 Frankfurt am Main, Germany.

Adrian Richter, Friedrich-Schiller-Universität Jena, Institut für Zoologie und Evolutionsforschung, 07743 Jena, Germany; Biodiversity and Biocomplexity Unit, Okinawa Institute of Science and Technology Graduate University, Onna-son, 904-0495, Okinawa, Japan.

Leonora Olivos-Cisneros, Laboratory of Social Evolution and Behavior, The Rockefeller University, New York, NY 10065, USA.

Thomas van de Kamp, Institute for Photon Science and Synchrotron Radiation (IPS), Karlsruhe Institute of Technology (KIT), Hermann-von-Helmholtz-Platz, 1, 76344 Eggenstein-Leopoldshafen, Germany; Laboratory for Application of Synchrotron Radiation (LAS), Karlsruhe Institute of Technology (KIT), Kaiserstr. 12, 76131 Karlsruhe, Germany.

Daniel J.C. Kronauer, Laboratory of Social Evolution and Behavior, The Rockefeller University, New York, NY 10065, USA; Howard Hughes Medical Institute, The Rockefeller University, New York, NY 10065, USA.

Rolf G. Beutel, Friedrich-Schiller-Universität Jena, Institut für Zoologie und Evolutionsforschung, 07743 Jena, Germany; Senckenberg Research Institute and Natural History Museum, Senckenberganlage 25, 60325 Frankfurt am Main, Germany.

Brendon E. Boudinot (contact author), Senckenberg Research Institute and Natural History Museum, Senckenberganlage 25, 60325, Frankfurt am Main, Germany; National Museum of Natural History, Smithsonian Institution, 10th & Constitution Ave. NW, 20560 Washington, DC, USA; Friedrich-Schiller-Universität Jena, Institut für Zoologie und Evolutionsforschung, 07743 Jena, Germany. E-mail: boudinotb@gmail.com; boudinotb@si.edu

Introduction

Larvae are the soft, fatty, and externally legless feeding stage of ants. Although the postcephalic tagmata of ant larvae are externally recognizable by subtle morphological cues, their bodies lack the clear constrictions, defensive structures, and sensory armature of adults, including long antennae and palps. The decoupling of adult and larval morphology is a defining feature of the Holometabola, allowing juveniles and adults to avoid direct competition through occupation of different spatial and trophic niches (Grimaldi & Engel 2005, Beutel & al. 2017), as observed in the sawflies ("symphyta"), parasitoids ("parasitica" plus Orussidae), and many Aculeata (stinging Hymenoptera) (e.g., Gauld & Bolton 1988). The larvae of eusocial Hymenoptera are peculiar, however, in that they are at once both individually helpless yet essential in the social context of the colony (Schultner & al. 2017). The larvae of ants are further unusual in that they are not kept in separate cells but are moved by workers either to food or to microenvironments within the nest that are most suitable for their development (Wheeler & Wheeler 1979, Tschinkel 2006). As a morphologically defined group within the colony, larvae perform the role of the "digestive caste" (Went & al. 1972, Wheeler & Wheeler 1979), both assimilating biomass for individual growth and storing food used by the collective in species with either trophallaxis or larval hemolymph feeding (Meurville & Leboeuf 2021, Negroni & Leboeuf 2023). The larval morphology of ants has received limited attention in the context of ant taxonomy, and even sparser attention in other contexts. Toward a more comprehensive knowledge of the form, function, and evolution of ant larvae, we perform here the first micro-computed tomographic (μ-CT) reconstruction of an ant larva, with comparisons across Formicidae, other Hymenoptera, and the Holometabola more broadly.

Two frameworks have developed over the past century for the study and interpretation of ant larval morphology. The first is based on external morphology, with comparative observations recorded for the purpose of improving the global classification of Formicidae. This system, rooted in the studies of, for example, Emery (1899) and Wheeler (1910, 1918), was constructed over several decades by George and Jeanette Wheeler, who codified patterns of consistent variation as terminologies for body profiles and mandible form, and outlined the central character list of size, shape, proportion, and position traits (Wheeler & Wheeler 1976, 1986; see also their references in Bolton 2024). The observational scope of this system is constrained to features that could be detected from whole specimens under alcohol or slide-mounted after staining and clearing (Wheeler & Wheeler 1961). Among these externally detectable characters are structures that are of functional significance in colony feeding. This includes the thoracic "food basket" of *Solenopsis invicta* (see Petralia & Vinson 1979, Tschinkel 2006: p. 349), the secretion-associated tubercles on the abdominal venter of some *Platythyrea* (Villet & al. 1990), the bizarre trophothylax of Pseudomyrmecinae (Wheeler 1918: figs. 7, 9), and the larval hemolymph tap of Leptanillinae (Wheeler 1928, Masuko 1989). This system, moreover, has recently been used as a morphological correlate for behavior in hypothesis tests indicating that enhanced control of larval feeding by workers is correlated with enhanced worker-queen dimorphism, among other traits relating to social complexity (Matte & Lebouef 2024).

The second framework emerges from numerous and mostly isolated studies on the internal anatomy of larvae, with limited phylogenetic or systematic scope but often answering particular questions with broader implications or direct utility for ant research. The need to identify whether larvae are reproductive- or worker-fated, for example, has revealed that larvae can be sexed based on their gonads (Ortius-Lechner & al. 2003), the count and distribution of genital imaginal discs (Penick & al. 2014) and crystalline deposits (Schultner & al. 2023), and in at least some cases, hair patterning (Adams & al. 2021), in addition to pigmentation pattern and body size (e.g., Rajakumar & al. 2024). Many studies conducted in this framework focus on one or two organ systems at a time, including the salivary and other head glands (Ofer 1970, Petralia & Haut 1986, Zara & Caetano 2002), the digestive tract (Weir 1957, Nitschmann 1959, Bonavita-Cougourdan & Poveda 1972, Solis & al. 2009), the nervous system (Weir 1959), the imaginal discs of the legs (Lappano 1958), the sting apparatus (Dewitz 1877), and the fat body (Jeantet 1969, Zara & al. 2004). A few studies have undertaken more comprehensive sampling of organ systems (Berlese 1902, Pérez 1902, Athias-Henriot 1947, Valentini 1951, Petralia & Vinson 1979). These studies have also documented the tracheae and musculature (Berlese 1902, Athias-Henriot 1947, Petralia & Vinson 1979), which are systems that have otherwise only been addressed coincidentally, if at all. Taken altogether, the studies under the second framework represent a scattershot of datapoints for comparative anatomy yet form a stronger basis for developmental and sociobiological research.

While no single technology is perfect for sampling the anatomy and morphology of any organism, studies on larvae are especially challenging due to the subjects' small and fragile bodies, the need for time-consuming and often damaging specimen preparation, and viewing planes restricted to slices or slides, limiting the possibility for measurement in the former and producing distortions in the latter. With this in mind, the central technical goal of the present study is to use synchrotron-radiation micro-computed tomography (SR-μ-CT) to document as much of the internal anatomy of a single ant larva as possible, complemented with scanning electron microscopy (SEM) for external morphology. Because the resolution of our SR-μ-CT scans is 1.22 μm, we are only able to address supracellular structures and tissues with these data, and we expect that the documentation of glandular systems is incomplete. We chose to focus our study on the clonal

raider ant, *Ooceraea biroi*, as this species has become a model organism for experimental biology (e.g., Hart & al. 2023, Frank & Kronauer 2024, Kronauer 2025).

The specific objectives of our study are: (1) to establish a new baseline for future anatomical studies of ant larvae by providing extensively annotated 3D renders with precise homology inferences; (2) to make the first larval-adult anatomical comparisons for Formicidae in the µ-CT-based framework established for adults (e.g., Richter & al. 2020, 2022, Boudinot & al. 2021); (3) to contextualize our observations with respect to key characters from Wheeler & Wheeler (e.g., 1976, 1986); and (4) to derive evolutionary morphological insights for the Formicidae and Hymenoptera more broadly from the comparison of ant larvae with other groups of Hymenoptera and Holometabola. By addressing objectives 1 - 3, we hope to unify the two frameworks for the study of larval anatomy and morphology, and for ants more broadly. Toward this end, we compare the larva of *Ooceraea biroi* with species for which anatomical information is available, and we extend comparisons to other species across the phylogeny by codifying eight characters from Wheeler and Wheeler for which we provide terminal plotting given recent phylogenomic insights (Romiguier & al. 2022). Our overarching goal is to stimulate research on larvae and morphogenesis in ants by providing a visual atlas of anatomy based on the foundation of µ-CT data. Although ant larvae may appear to be simple, sausage-shaped life forms, their structural complexity and social importance is remarkable both instantaneously and through time.

Material and methods

Specimens and preparation

Ooceraea biroi stock colonies from clonal line B (Kronauer & al. 2012) were used for all experiments. Regarding the identification of *O. biroi* clonal lines, see also Trible & al. (2020), in which the phylogeographic and invasive history of the species was reconstructed. Stock colonies were fed with frozen fire ant (*Solenopsis invicta*) brood and escamoles (*Liometopum* sp.) and were maintained in environmental rooms at 25 °C in closed plastic containers with a plaster of Paris floor. Specimens were preserved directly into 100% ethanol for scanning; all material from this study is deposited in the Senckenberg Naturmuseum Frankfurt Hymenoptera collection (SMFH).

Scanning Electron Microscopy

The third instar larvae were dehydrated stepwise in ethanol (70% to 100%), subsequently transferred to acetone and dried at the critical point in liquid CO_2 with an EMITECK K850 Critical Point Dryer (Quorum Technologies Ltd., Ashford, UK). The samples were glued onto a microneedle and placed on a rotatable specimen holder (Pohl 2010). Sputter coating with gold was applied with an EMITECK K500 (Quorum Technologies Ltd.). SEM micrographs were taken with a ESEM XL30 (Philips, Amsterdam, the Netherlands).

Micro-computed tomography scanning and visualization

Specimens of the third instar were scanned at the high-throughput X-ray microtomography setup at the IMAGING CLUSTER at KIT Light Source (Karlsruhe Institute of Technology). A parallel polychromatic X-ray beam produced by a 1.5 T bending magnet was spectrally filtered by 0.5 mm aluminum to remove low energy components from the beam. The resulting spectrum had a peak at about 15 keV, and a full width at half maximum bandwidth of about 10 keV. Unstained specimens in ethanol were scanned at a magnification of 10 x, resulting in an effective pixel size of 1.22 µm. A fast indirect detector system was utilized, consisting of a 13 µm Terbium-doped Lu_2SiO_5 (LSO) scintillator (Cecilia & al. 2011), a diffraction limited optical microscope (Optique Peter, Lentilly, France) (Douissard & al. 2012) and a 12-bit pco.dimax S4 high-speed camera (Excelitas PCO GmbH, Kehlheim, Germany) with a resolution of 2016 × 2016 pixels. Each scan included the acquisition of 200 dark field images, 200 flat field images, and 3000 equiangularly spaced radiographic projections in a range of 180° with 10 milliseconds exposure time each, resulting in a scan duration of 34 seconds. The control system concert (Vogelgesang & al. 2016) was employed for automated data acquisition and online reconstruction of tomographic slices for data quality assurance. The final tomographic 3D reconstruction was performed by tofu (Faragó & al. 2022) and included phase retrieval (Paganin & al. 2002), ring removal, 8-bit conversion, and blending of phase and absorption 3D reconstructions in order to increase contrast between the background and homogeneous regions, while at the same time highlighting the edges.

From the raw scan data of multiple specimens, individuals were separated using the cropping editor of Amira 6.0 (Visage Imaging GmbH, Berlin, Germany). The target specimen was presegmented by marking each part of the whole body at every 30th slice. These presegmentations were then semiautomatically completed using the algorithm of Biomedisa (Lösel & al. 2020), then manually corrected and exported using the Multiexport function of Amira (Engelkes & al. 2018). Exported TIFF image stacks were imported into VG Studio Max 3.4 (Volume Graphics, Heidelberg, Germany) to create volume renderings using Phong shading.

Drawings

Drawings were made using volume renders based on µ-CT data and SEM micrographs and digitized using Adobe Illustrator 2021 software (Adobe, San Jose, CA, USA).

Image processing

All figures and labels were processed and composed in Adobe Illustrator 2021 (Adobe Systems, San Jose, CA).

Terminology

The terminology is generally based on Beutel & al. (2008, 2014), which is largely compatible with the Hymeno-

ptera Anatomy Ontology (HAO; Yoder & al. 2010). The terms for chaetotaxy of the head are based on Hinton's (1946) work on the homology and nomenclature of setae of lepidopteran larvae. Shape terminology for larval bodies, heads, mandibles, and selected other structures are drawn from the work of Wheeler & Wheeler (1976, 1986).

The muscular nomenclature follows von Kéler (1963) and Beutel & al. (2008, 2014), which is a terminology covering the entire Neoptera with many previous applications to various groups of insects including hymenopteran larvae (Beutel & al. 2008). Following von Kéler (1963), the description includes the origin (**O**), insertion (**I**), and also the function (**F**) of each muscle. Additionally, size shape and configuration (**S**) are also added. To reduce possible ambiguities, homology-neutral labels of head muscles are presented first (e.g., "M. 7") (from Beutel & al. 2008), then followed by the numerical labels (e.g., "M.' 1") from Short (1951), and finally, homology-explicit labels (e.g., "0lb5") of Beutel & al. (2014) were added. For the postcephalic musculature, the topographic main-group system for muscle naming is based on Beutel & al. (2014): (1) dorsal longitudinal muscles, which originate and insert both on dorsal regions of segments (" / **II** / **IIIdlm**" for thoracic muscles and "**dlmI** / **II** / ... / **X**" for abdominal muscles); (2) ventral longitudinal muscles, which originate and insert on ventral regions of segments ("**I** / **II** / **IIIvlm**" for thoracic muscles and "**vlmI** / **II** / ... / **X**" for abdominal muscles); (3) dorsoventral muscles, which are dorsoventrally orientated ("**I** / **II** / **IIIdvm**" for thoracic muscles and "**dvmI** / **II** / ... / **X**" for abdominal muscles); and (4) anal muscles (**anm**).

Morphological character mapping

To illustrate the diversity of ant larval morphological traits across a phylogenetic framework, eight key morphological characters were mapped onto the phylogenomic result of Romiguier & al. (2022). The purpose of mapping the morphological traits of Wheeler and Wheeler onto the phylogenetic tree is not to infer evolutionary relationships or construct a phylogeny based on these traits. Instead, it serves to visualize the diversity and distribution of morphological characteristics across known lineages, based on a robust phylogeny.

Eight characters were scored across 217 taxa from previous literature, primarily from Wheeler & Wheeler (1976, 1986), as well as from Yamada & al. (2020) for *Opamyrma*, Wheeler & Wheeler (1957) for *Simopelta*, Wheeler & al. (1980) for *Nothomyrmecia*, and Wheeler & Bailey (1920) for Pseudomyrmecinae. See Wheeler & Wheeler (1957, 1976, 1986) for illustrations and definitions of the body forms and mandibles.

1. Body form, categories *sensu* Wheeler & Wheeler (1976, 1986) in aggregate: (**0**) "leptanilloid"; (**1**) "pogonomyrmecoid"; (**2**) "myrmecioid"; (**3**) "aphaenogastroid"; (**4**) "platythyreoid"; (**5**) dolichoderoid"; (**6**) "crematogastroid"; (**7**) "leptomyrmecoid"; (**8**) "pheidoloid"; (**9**) "oecophylloid"; (**10**) "attoid"; (**11**) "paedalgoid"; (**12**) "rhopalomastigoid"; (**13**) "simpeltoid" (for this term, see Wheeler & Wheeler 1957).
2. Mandible form, categories *sensu* Wheeler & Wheeler (1976): (**0**) "leptanilloid"; (**1**) "amblyoponoid"; (**2**) "ectatommoid"; (**3**) "dinoponeroid"; (**4**) "typhlomyrmecoid"; (**5**) "platythyreoid"; (**6**) "diacammoid"; (**7**) "pogonomyrmecoid"; (**8**) "pristomyrmecoid"; (**9**) "leptogenydoid"; (**10**) "cephalotoid"; (**11**) "attoid"; (**12**) "dolichoderoid"; (**13**) "simoponoid"; (**14**) "tetraponeroid"; (**15**) "camponotoid"; (**16**) "rhytidoponeroid"; (**17**) "pheidoloid".
3. Leptanilline protuberance, which is also known as ventral prothoracic projection or process in Leptanillinae, see Wheeler & Wheeler (1976): (**0**) absent; (**1**) present.
4. Trophothylax (a pocket behind the mouth, where the workers place food), *sensu* Wheeler & Bailey (1920): (**0**) absent; (**1**) present.
5. Mandibular ridges: (**0**) absent; (**1**) present.
6. Chiloscleres (a pair of conspicuous dark brown sclerotized spots, located on either side of the labrum): (**0**) absent; (**1**) present.
7. Praesaepium (shallow depression on the ventral surface of certain anterior abdominal segments): (**0**) absent; (**1**) present.
8. Body tubercles: (**0**) absent; (**1**) > 2 present laterally; (**2**) > 2 present ventrally; (**3**) one pair present; (**4**) present, in the form of bosses.

Results

Description of external and internal morphology

General appearance: The grub-like penultimate larval instar we examined is approximately 1 mm long (Fig. 1). The head is large and subglobular (Fig. 2). The postcephalic body is "myrmecioid" in silhouette *sensu* Wheeler & Wheeler (1976: p. 7), that is, it appears approximately cylindrical and slightly curved in lateral view, widening in the posterior half of the abdomen, and terminating with abdominal segment X, which is rounded-conical. The cuticle is whitish, largely unpigmented, with only the cephalic appendages appearing slightly darker. The prothorax is distinctly longer than all other postcephalic segments. The borders of the thoracic and abdominal segments are disconnected laterally, most distinctly between the pro- and mesothorax, that is, the segmental connections are zigzag-shaped. The thoracic legs and abdominal appendages are absent externally, and protuberances are not developed. The sclerotized cuticular regions of the head are largely smooth and equipped with a moderately dense vestiture of setae. In contrast, the surface of the postcephalic body appears weakly sclerotized and wrinkled and bears numerous setae and a very dense pattern of microtrichiate squamae, that is, serrated scale-like structures, with the cuticle smoothing out in the terminal two segments (AIX, AX). The "*Leptanilla* protuberance", the trophothylax, chiloscleres, and the praesaepium (all *sensu* Wheeler & Wheeler 1976) are absent.

Chaetotaxy: The head bears a vestiture of setae and sensilla similar to what is found in other holometabolous

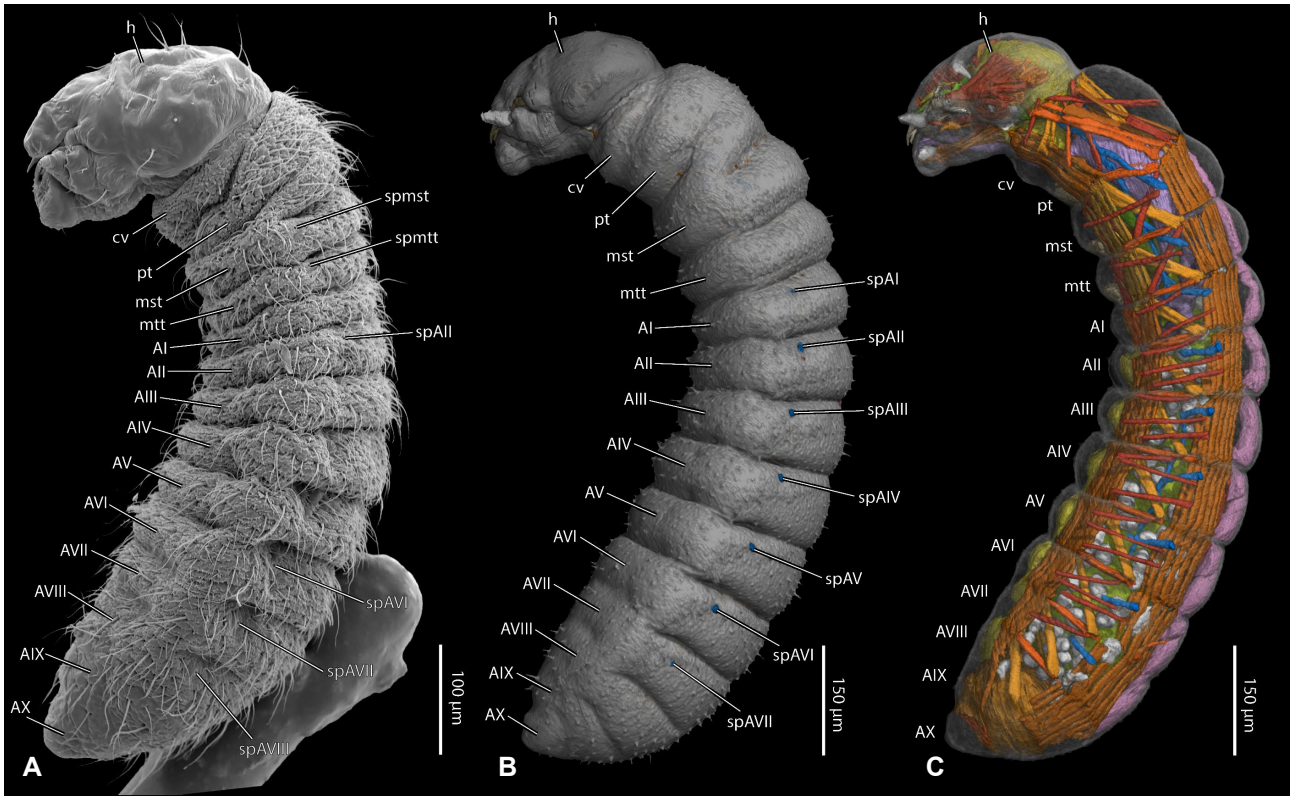

Fig. 1: Third instar larva of *Ooceraea biroi*, lateral view. **A:** scanning electron microscopy image; **B, C:** 3D reconstruction. – ***Abbreviations*: cv:** cervical membrane; **h:** head; **mst:** mesothorax; **mtt:** metathorax; **pt:** prothorax; **spmst:** mesothoracic spiracle; **spmtt:** metathoracic spiracle; **spAI - spAVIII:** abdominal spiracles I - VIII; **AI - AX:** abdominal segments I - X.

larvae (Figs. 3, 4) (e.g., *Caurinus* [Mecoptera], Fabian & al. 2015; Lepidoptera, Hasenfuss & Kristensen 2003: fig. 5.3B). Two pairs of long setae (ca. 70 µm) are present on the middle frontal area (AF_1, AF_2) and three along a transverse fold of the anteriormost frontal region (F_1, A_1, A_2). The homology of a very short spine-like structure below and laterad the insertion of A_1 is unclear. Three paired long setae are arranged in an oblique row on the vertexal area (V_{1-3}). Additionally, one seta is inserted on the genal region at the area of the maximum width of the head capsule (L); two are below the vestigial antennae ($O_{1, 2}$), and one is situated on the lower genal region (SO_2). Three medium length setae (ca. 30 µm) are arranged in an oblique row on the anterior clypeal region (C_{1-3}). A long seta is present on the cardo (Ca_1) and two of medium length on the stipital region (St_{1-2}). A single medium length seta is inserted on the proximal prementum (Pm_1) and three very short setae above it, two anterolaterad of it, and one anteromesad (Pm_{2-4}). The labrum, the vestigial antennae, and the mandibles lack setae. Numerous long setae are inserted on the thorax and abdominal segments I - VIII, without an easily recognizable pattern. The setation is less dense on segment IX, and only two short setae are present laterally on segment X.

Head: Head capsule (Figs. 2 - 5). The large orthognathous head is ca. 0.3 mm long from the posterior vertexal region to the tip of the labrum, and its maximum width in the middle cephalic region is ca. 0.2 mm. It is subglobular and approximately subhexagonal *sensu* Wheeler & Wheeler (1976: p. 30); it is very slightly compressed antero-posteriorly, distinctly convex dorsally and frontally, but rather flat on the posterior side, which is largely formed by the labium. The entire head capsule is only moderately sclerotized and whitish; only two pairs of appendages or endite lobes are easily discernible and pigmented, the mandibles and maxillary galeae. The sclerotized surface areas of the head capsule are evenly curved (regions of unevenness in SEM micrographs are artefacts) and largely smooth; in contrast, semimembranous or membranous regions have a strongly sculptured surface, with large and irregular tubercular or scale-like structures. The system of sutures and ridges is distinctly reduced; oblique, posteriorly converging frontoclypeal ridges are present; their posterior ends are covered by the median part of a distinct transverse fold of the anterior frontal region; the anterior tentorial grooves are visible anterior to this area; the epicranial ecdysial sutures, that is, the frontal sutures and the coronal suture, are strongly reduced, scarcely recognizable as indistinct zones of weakness; the clypeolabral suture is largely reduced, only indistinctly recognizable as a faint transverse ledge. A gula or a hypostomal or postgenal bridge are not developed.

Internal skeletal structures (Fig. 5D: ata, tb). The tentorium is well-developed. The anterior arms are elongated and slightly inflated anteriorly. The fissure-shaped anterior tentorial pits are clearly visible paramedially on

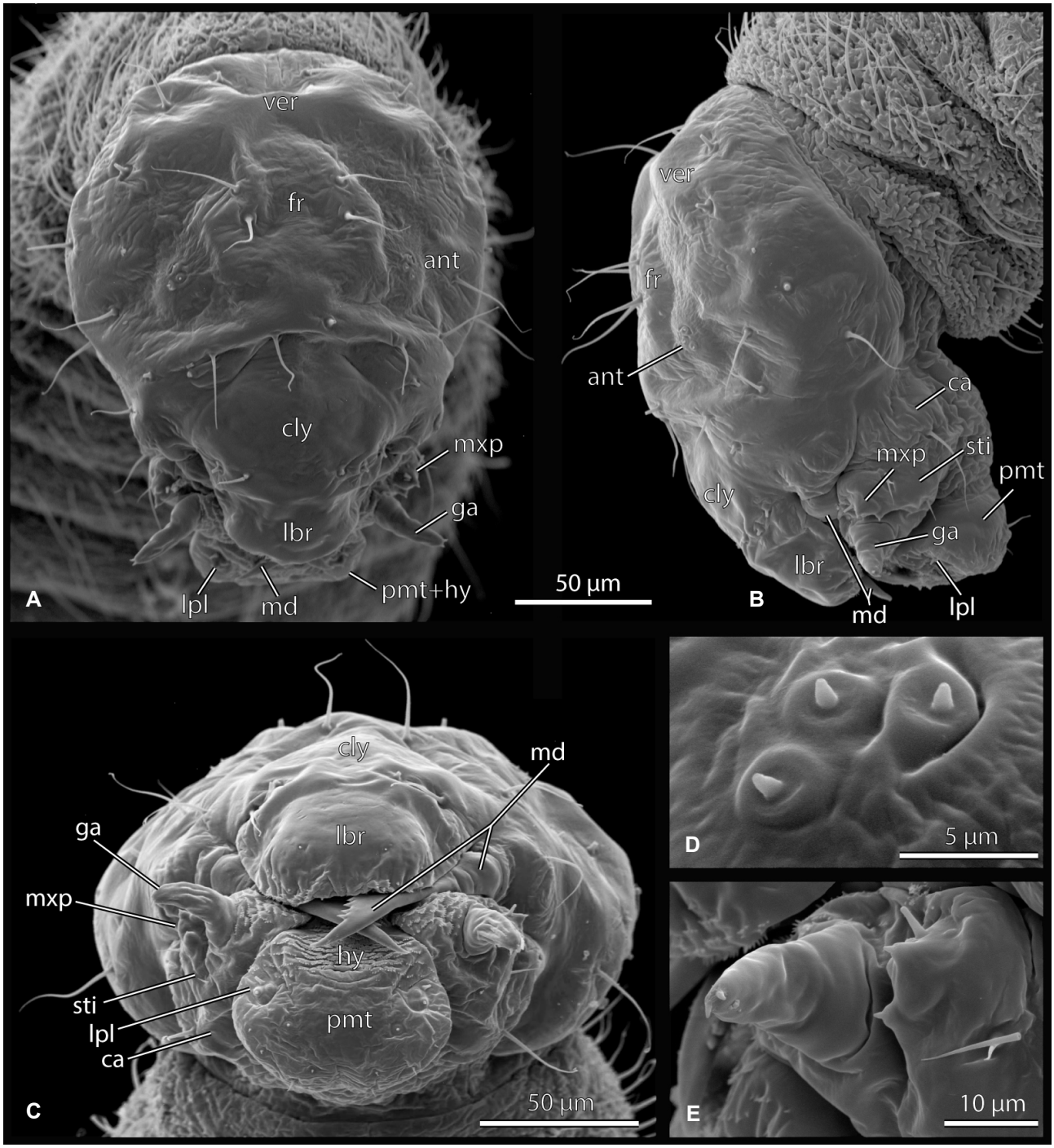

Fig. 2: Scanning electron microscopy micrographs of the 3rd instar larval head of *Ooceraea biroi*. **A:** dorsal view; **B:** lateral view; **C:** frontal view; **D:** vestigial antennae; **E:** galea and vestigial maxillary palp. – ***Abbreviations*: ant:** antennae; **ca:** cardo; **cly:** clypeus; **fr:** frontal area; **ga:** galeae; **hy:** hypopharynx; **lbr:** labrum; **lpl:** labial palp; **md:** mandible; **mxp:** maxillary palp; **sti:** stipes; **pmt:** prementum; **ver:** vertexal area.

the border between the clypeus and frontal area. The dorsal arms are apparently vestigial or missing (not recognizable in µ-CT data). The posterior arms are short and thick, connected by a massive transverse bridge. The distinct posterior pits are located at the posterolateral end of the postmentum, close to the cervical membrane.

Stemmata. Stemmata are not recognizable and apparently completely reduced.

Labrum (Figs. 2, 5). The labrum appears like a fleshy lobe. It is slightly narrower than the clypeus, with which it is largely fused. It is laterally rounded, and its distal margin is slightly convex, thus it is semicircular in form *sensu* Wheeler & Wheeler (1976: p. 37). It entirely lacks setae. Three spine-like sensilla are arranged in a row near the lateral edge in frontal view. The distal region appears slightly folded and bears some small, serrated scale-like

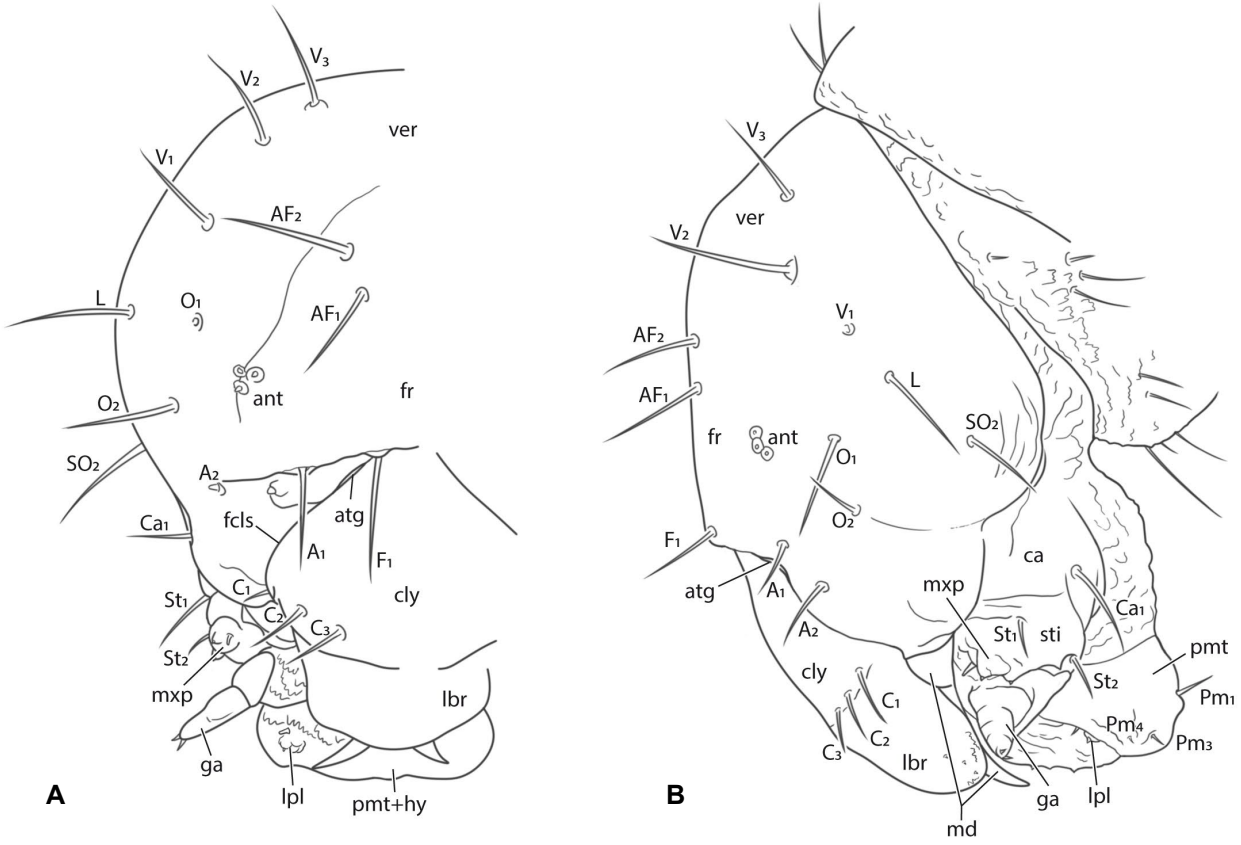

Fig. 3: Chaetotaxy of the 3rd instar larval head of *Ooceraea biroi*. **A:** dorsal view; **B:** lateral view. – ***Abbreviations*: ant:** antennae; **atg:** anterior tentorial grooves; **ca:** cardo; **cly:** clypeus; **fcls:** frontoclypeal suture; **fr:** frontal area; **ga:** galeae; **hy:** hypopharynx; **lbr:** labrum; **lpl:** labial palp; **md:** mandible; **mxp:** maxillary palp; **pmt:** prementum; **sti:** stipes; **ver:** vertex; chaetotaxy terms as in section Chaetotaxy.

structures. **Musculature of labrum.** The intrinsic labral muscle is present, whereas both extrinsic muscles are missing. ***M. labroepipharyngalis* (M. 7 / M.' 1 / 0lb5): S** (= size, shape, and general configuration): one or two vertical bundles; **O** (= origin): central area of dorsal labral wall; **I** (= insertion): centrally on anterior epipharynx; **F** (= inferred function): levator of anterior epipharynx. ***M. frontolabralis* (M. 8 / M.' 2 / 0bl1):** Absent. ***M. frontoepipharyngalis* (M. 9 / M.' 3 / 0bl2):** Absent.

Antenna (Fig. 2). The antennae are vestigial, represented by a group of three rounded papillae situated on a low disc, each equipped with a minute spine-like sensillum; they are situated in the lower third of the head capsule (excl. the mouthparts). **Musculature of antenna.** All extrinsic and intrinsic antennal muscles are absent. ***M. tentorioscapalis anterior* (M. 1 / M.' 5 / 0an1):** Absent. This muscle is likely equivalent to M.' 5 of Short (1951) considering its relatively medial position. ***M. tentorioscapalis posterior* / *lateralis* / *medialis* (Mm. 2 - 4 / M.' 4 / 0an2 - 4):** Absent. Likely equivalent to M.' 4 of Short (1951) considering its relatively lateral position. ***Mm. scapopedicellaris lateralis* / *medialis* (Mm. 5 / 6 / X / ?):** Absent. Not included in Short (1951).

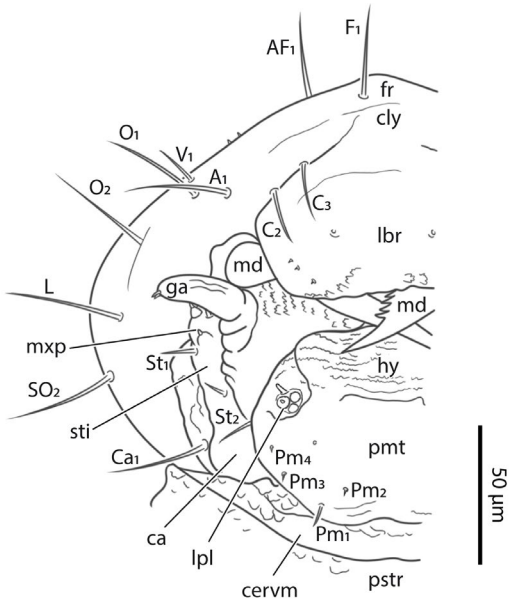

Fig. 4: Chaetotaxy of the 3rd instar larval head of *Ooceraea biroi*, frontal view. – ***Abbreviations*: ca**: cardo; **cervm**: cervical membrane; **cly**: clypeus; **fr**: frontal area; **ga**: galeae; **hy**: hypopharynx; **lbr**: labrum; **lpl**: labial palp; **md**: mandible; **mxp**: maxillary palp; **pmt**: prementum; **sti**: stipes; chaetotaxy terms as in section Chaetotaxy.

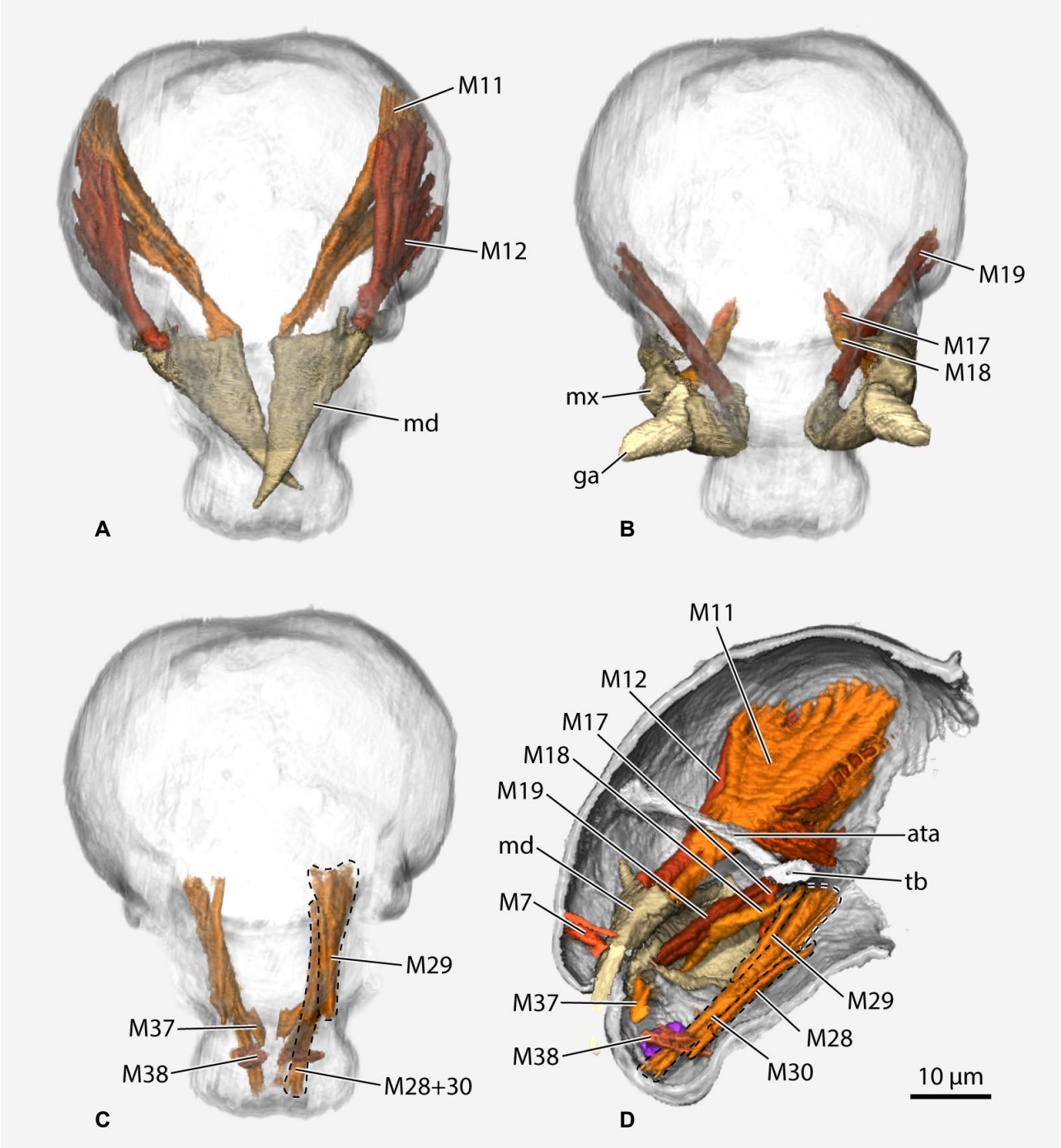

Fig. 5: 3D reconstruction of the 3rd instar larval head of *Ooceraea biroi*, emphasizing skeletal and muscular elements. **A, B, C:** dorsal view; **D:** sagittal view. **A:** mandibular musculature; **B:** maxillary musculature; **C:** labial and salivary musculature; **D:** mandibular, maxillary, labral, and labial musculature. – ***Abbreviations*: ata:** anterior tentorial arm; **ga:** galeae; **md:** mandible; **mx:** maxillae; **tb:** tentorial bridge; **M7:** *M. labroepipharyngalis*; **M11:** *M. craniomandibularis internus*; **M12:** *M. craniomandibularis externus*; **M17:** *M. tentoriocardinalis*; **M18:** *M. tentoriostipitalis*; **M19:** *M. craniolacinialis*; **M28:** *M. submentopraementalis*; **M29:** *M. tentoriopraementalis inferior*; **M30:** *M. tentoriopraementalis superior*; **M37:** *M. hypopharyngosalivaris*; **M38:** *M. praementosalivaris anterior.*

Mandible (Figs. 2, 5). The ventromedially directed mandibles are well-developed, slightly asymmetrical, relatively broad basally and tapering distally (Figs. 2, 5); they are "amblyoponoid" in form, *sensu* Wheeler & Wheeler (1976: p. 40), that is, narrowly subtriangular, without a blade, with the apex slightly curved mesad, and with small teeth on the medial border. The mandibular base, which is partly exposed, is articulated in a dicondylic manner, with the dorsal secondary joint less strongly developed than the ventral primary one. *In*

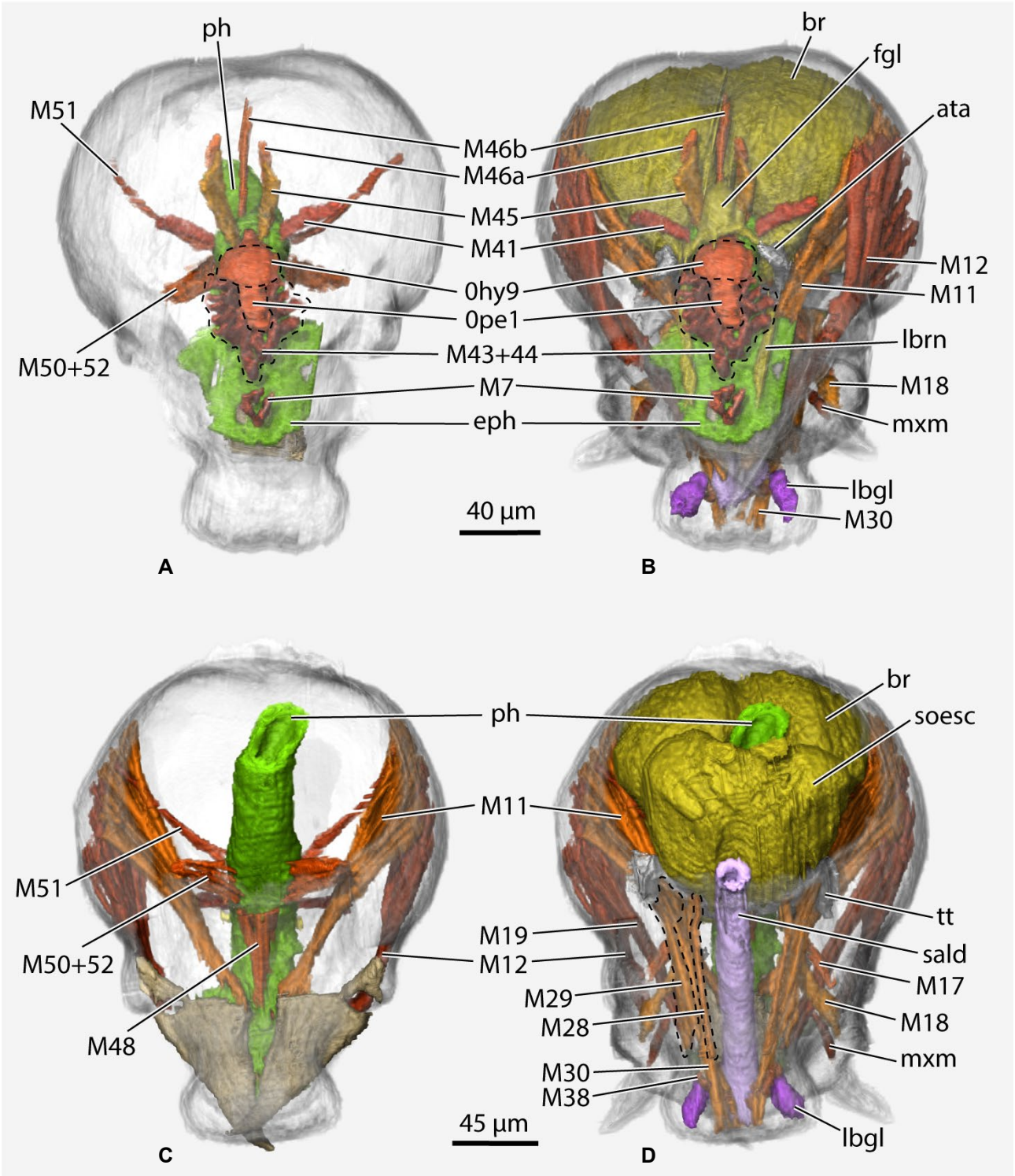

Fig. 6: 3D reconstruction of the 3rd instar larval head of *Ooceraea biroi*, emphasizing pharyngeal, nervous system, and salivary elements. **A, B:** dorsal view; **C, D:** ventral view; **A:** pharyngeal musculature; **C:** mandible and pharyngeal musculature; **B, D:** cephalic musculature, digestive tract, glands, and the central nervous system. – ***Abbreviations*: ata:** anterior tentorial arm; **br:** brain; **eph:** epipharynx; **fgl:** frontal ganglion; **lbgl:** labial gland; **lbrn:** labral nerve; **mxm:** maxillary muscles; **ph:** pharynx; **sald:** salivary duct; **soesc:** suboesophageal complex; **tt:** tentorium; **M7:** *M. labroepipharyngalis*; **M11:** *M. craniomandibularis internus*; **M12:** *M. craniomandibularis externus*; **M17:** *M. tentoriocardinalis*; **M18:** *M. tentoriostipitalis*; **M19:** *M. craniolacinialis*; **M28:** *M. submentopraementalis*; **M29:** *M. tentoriopraementalis inferior*; **M30:** *M. tentoriopraementalis superior*; **M38:** *M. praementosalivaris anterior*; **M41:** *M. frontohypopharyngealis*; **M43:** *M. clypeopalatalis*; **M44:** *M. clypeobuccalis*; **M45:** *M. frontobuccalis anterior*; **M46:** *M. frontobuccalis posterior*; **M48:** *M. tentoriobuccalis anterior*; **M50:** *M. tentoriobuccalis posterior*; **M51:** *M. verticopharyngalis*; **M52:** *M. tentoriopharyngalis*; **0hy9:** *M. pharyngoepipharyngalis*; **0pe1:** *M. oralis transversalis*.

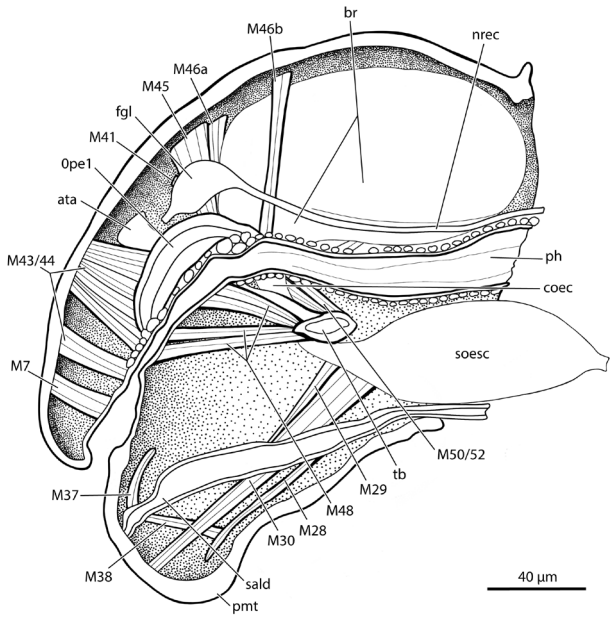

Fig. 7: The 3rd instar larval head of *Ooceraea biroi*, sagittal view. – ***Abbreviations*: ata:** anterior tentorial arm; **br:** brain; **coec:** circumoesophageal connective; **fgl:** frontal ganglion; **nrec:** nervus recurrens; **ph:** pharynx; **sald:** salivary duct; **soesc:** suboesophageal complex; **pmt:** prementum; **tb:** tentorial bridge; **M7:** *M. labroepipharyngalis*; **M28:** *M. submentopraementalis*; **M29:** *M. tentoriopraementalis inferior*; **M30:** *M. tentoriopraementalis superior*; **M37:** *M. hypopharyngosalivaris*; **M38:** *M. praementosalivaris anterior*; **M41:** *M. frontohypopharyngealis*; **M43:** *M. clypeopalatalis*; **M44:** *M. clypeobuccalis*; **M45:** *M. frontobuccalis anterior*; **M46:** *M. frontobuccalis posterior*; **M48:** *M. tentoriobuccalis anterior*; **M50:** *M. tentoriobuccalis posterior*; **M52:** *M. tentoriopharyngalis*; **0pe1:** *M. oralis transversalis.*

situ, the middle region of the mandible is covered by the fleshy labrum, with only approximately the distal third visible; the exposed slender distal part bears a long and apically pointed tooth and at least four sharp, triangular subapical teeth, distinctly separated from the mandibular apex by a nearly straight cutting edge. A basal mola is missing. The surface of the mandible appears smooth; surface ridges are not recognizable (on SEM images). **Musculature of mandible.** The cranial adductor and abductor are well-developed, whereas the smaller mandibular muscles with a tentorial or hypopharyngeal origin are absent. ***M. craniomandibularis internus* (M. 11 / M.' 9 / 0md1): S:** a bundle of voluminous muscles, subdivided into two subcomponents; **O:** dorsolateral and posterolateral areas of the head capsule; **I:** medially on the mandibular base with a well-developed tendon; **F:** mandibular adductor. ***M. craniomandibularis externus* (M. 12 / M.' 8 / 0md3): S:** a large muscle divided into two subcomponents; **O:** dorsolateral and posterolateral areas of the head capsule, laterad the origin of M. 11; **I:** laterally on the mandibular base with a tendon; **F:** mandibular abductor. ***M. hypopharyngo-mandibularis* (M. 13) / *M. tentoriomandibularis medialis inferior* (0md8):** Absent.

Maxillae (Figs. 2, 5). The maxillae are well-developed and inserted in deep maxillary grooves, laterad and above the labium. The large cardo has a somewhat folded surface and is at least partly fused with the lower edge of the genal region. The border with the stipes is irregular. The stipes is smaller than the cardo and its surface is largely smooth and sclerotized; it forms a structural unit with the highly modified unsegmented maxillary palp, which is in the form of a skewed peg *sensu* Wheeler & Wheeler (1976: p. 42), that is, it is produced as a lobe with a sinuate profile; it displays an irregular arrangement of rounded protuberances with spine-like sensilla of different size; its dorsal surface is separated from the stipital surface by a deep narrow fold. The galea is well-developed and appears palp-like; it is digitiform *sensu* Wheeler & Wheeler (1976: p. 42); apically, it bears two short, conical sensilla. **Musculature of maxillae.** Three of four extrinsic maxillary muscles are present; all intrinsic muscles are missing. ***M. craniocardinalis externus* (M. 15 / M.' 10 / 0mx1):** Absent. ***M. tentoriocardinalis* (M. 17 / M.' 11 / 0mx3): S:** two parallel bundles; **O:** anteroventrally on the intersection of the anterior tentorial arm and the tentorial bridge; **I:** laterally on the base of the cardo; **F:** adductor of the maxilla. ***M. tentoriostipitalis* (M. 18) / *M. tentoriostipitalis anterior* (0mx4) (Mm.' 12, 13a, 13b): S:** a bundle with horizontal orientation; **O:** below the origin of M. 17; **I:** posterior region of the stipes; **F:** adductor of the maxilla. ***M. craniolacinialis* (M. 19 / M.' 15 / 0mx2): S:** a well-developed muscle with a horizontal orientation; **O:** posterior region of the head capsule, below the areas of origin of M. 11 and M. 12; **I:** deeply within the maxillary lumen; **F:** adductor of lacinia / maxilla. ***M. stipitolacinialis* (M. 20 / M.' 15 / 0mx6):** Absent. ***M. stipitopalpalis externus* (Mm. 22 / 23 / Mm.' 17, 18):** Absent. ***Mm. palpopalpalis primus, secundus, tertius* (Mm. 24 - 27):** Absent. **Note:** Short (1951) observed 0mx1 (his M.' 10) in the wood wasp *Xiphydria*. In this genus, Short (1951) also recognized three tentoriostipital muscles (M.' 12 = "proximal stipes adductor", M.' 13a = "first distal stipes adductor", M.' 13b = "second distal stipes adductor") and two stipitopalpal muscles (M.' 17 = "maxillary palp adductor", M.' 18 = "maxillary palp depressor"). **Note:** We identified a short structure, probably a muscle bundle, and likely part of M18, or less likely M19 with modified insertion (Fig. 3B, C: mxm).

Labium (Figs. 2, 5). The labium is composed of two major elements, a nearly flat and undivided postmentum and a voluminous but structurally undifferentiated, cushion-like prementum. The postmentum is unsclerotized and has a rough tubercular surface structure. The prementum is placed below the mandibles and its lateral portions are enclosed by the maxillae; it is sclerotized, and its ventral and lateral areas are smooth, whereas its anterior surface appears moderately wrinkled. The labial palps are vestigial, represented by a group of three rounded papillae

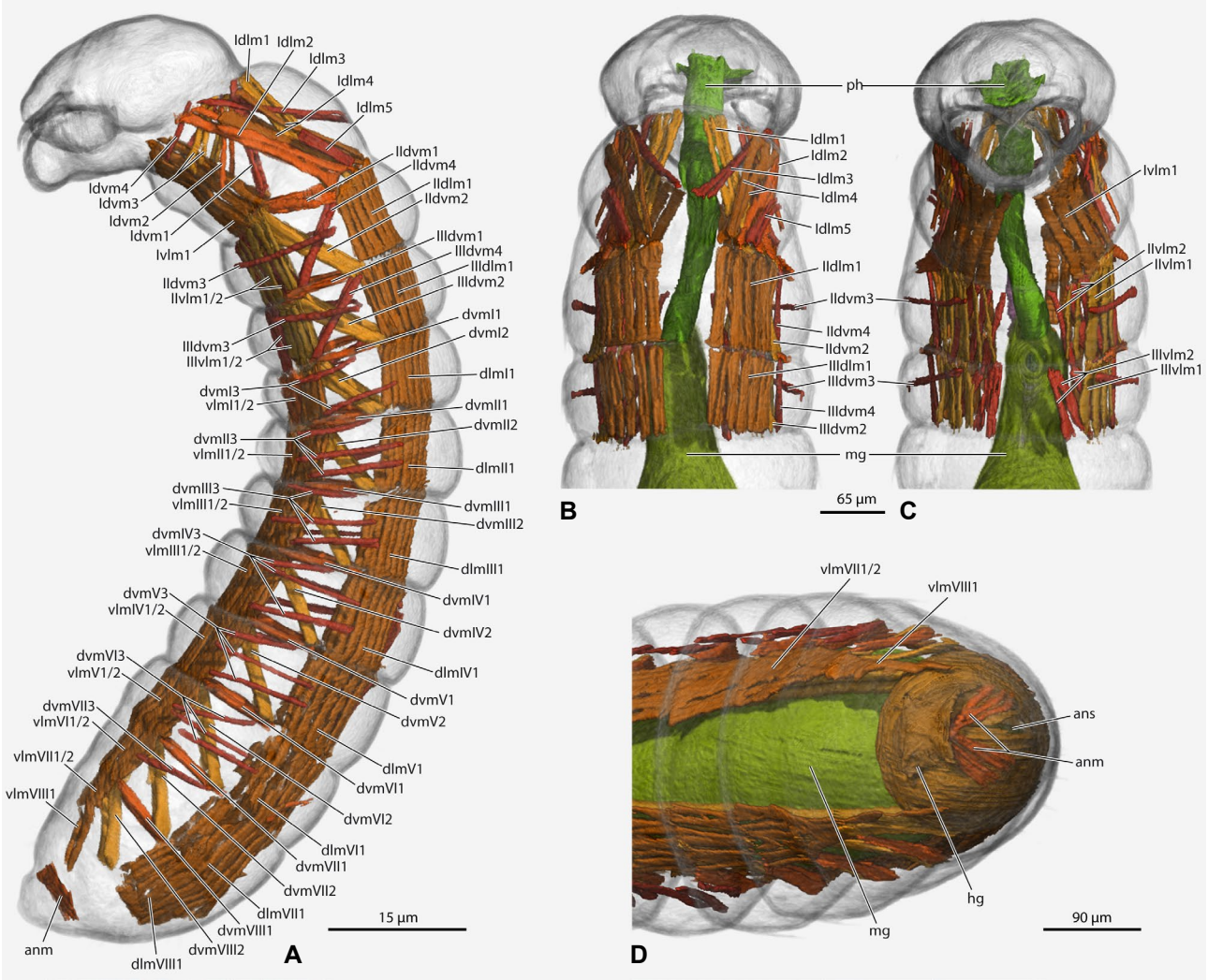

Fig. 8: 3D reconstruction of the 3rd instar larval postcephalic musculature of *Ooceraea biroi*. **A:** postcephalic musculature, lateral view; **B:** thorax, dorsal view; **C:** thorax, ventral view; **D:** abdominal segments VII - X, ventral view. – ***Abbreviations*: anm:** anal muscles; **ans:** anus; **hg:** hindgut; **mg:** midgut; **ph:** pharynx; numbering of the muscles as in section Thorax and section Abdomen.

situated on a low disc, only with the lateral one of them bearing a minute spine-like sensillum; a small, cylindrical sensillar process is present above the group. Labial endite lobes are absent. The anterior hypopharynx is largely integrated into the voluminous anterior labium (see below) but is distinctly characterized by its surface, which is formed by somewhat irregular and interrupted transverse folds densely set with minute spines. **Musculature of labium.** All three premental retractors are present, but intrinsic muscles of the prementum are absent (Fig. 5). ***M. submentopraementalis* (M. 28 / ? / 0la8): S:** a pair of slender muscles with horizontal orientation; **O:** proximolateral submental region of the postmentum; **I:** distal part of prementum; **F:** premental retractor. ***M. tentoriopraementalis inferior* (M. 29 / M.' 23 / 0la5): S:** a well-developed muscle with horizontal orientation; **O:** anteroventrally on the posterior tentorial arm; **I:** lateral premental region; **F:** levator of the prementum. ***M. tentoriopraementalis superior* (M. 30 / M.' 24 / 0la6): S:** a well-developed elongate muscle with horizontal orientation, mesad M. 29; **O:** anteroventrally on the posterior tentorial arm, mesad M. 29; **I:** anterior wall of prementum; **F:** retractor of the prementum. ***M. praementopalpalis internus / externus* (M. 33 / 34):** Absent. ***M. palpopalpalis labii primus / secundus* (M. 35 / 36):** Absent. ***M. tentoriohypopharyngalis* (M. 42 / M.' 24 / 0hy3):** Absent. **Note:** Muscles "*rst a*" and "*rst b*" of Parker (1935) are difficult to align and their homology with muscles of *Xyela* (Beutel & al. 2008) is presently unclear. Parker (1935) did not identify muscles of the labial palps.

Cephalic digestive tract (Fig. 6). The cibarium forms an angle of slightly more than 90° with the pharynx. The anterior half of the epipharynx is flat and continuous with the short ventral wall of the labrum. The anterior hypopharynx is slightly convex and fused to the dorsal wall of the anterior labium. The laterally open anterior half of the cibarium is about half as broad as the head capsule in this region; the posterior part is a closed prepharyngeal tube formed by fusion of the lateral edges of the posterior

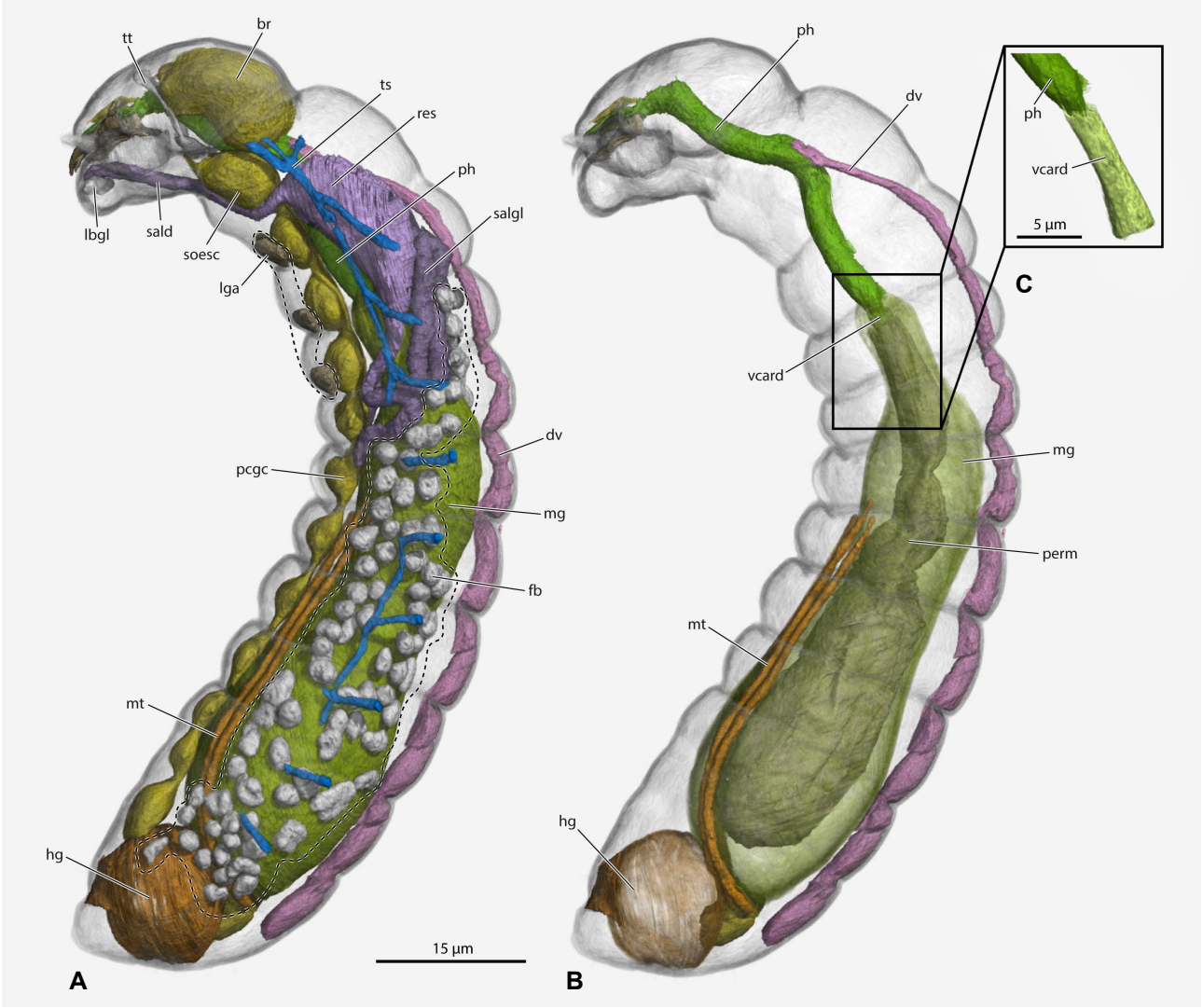

Fig. 9: 3D reconstruction of the 3rd instar larva of *Ooceraea biroi*, lateral view. **A:** dorsal vessel, fat body, gland, salivarium, and digestive, nervous, and tracheal systems; **B:** digestive system and dorsal vessel; **C:** valvula cardiaca inside the peritrophic membrane. – ***Abbreviations*: br**: brain; **dv**: dorsal vessel; **fb**: fat body; **hg**: hindgut; **lbgl**: labial gland; **lga**: leg imaginal discs (leg anlagen); **mg**: midgut; **mt**: Malpighian tubules; **pcgc**: postcephalic ganglionic chain; **perm**: peritrophic membrane; **ph**: pharynx; **res**: reservoir; **sald**: salivary duct; **salgl**: salivary gland; **soesc**: suboesophageal complex; **ts**: tracheal system; **tt**: tentorium; **vcard**: valvula cardiaca.

epi- and hypopharynx; this section is only about half as wide as the anterior cibarium, similar in width to the tube-like pharynx; it is curved upwards laterally, with the dorsolateral edges serving as attachment areas for the transverse prepharyngeal muscles. **Musculature of digestive tract.** Eight of nine muscles normally associated with the cephalic digestive tract are present. ***M. frontohypopharyngealis* / *M. frontooralis* (M. 41 / ? / 0hy1): S:** well-developed; **O:** middle frontal region; **I:** dorsolaterally on the anatomical mouth, immediately close to the frontal ganglion; **F:** levator and dilator of the anatomical mouth. ***M. clypeopalatalis* (M. 43 / Mm.' 33, 34 / 0ci1): S:** three small bundles; **O:** central clypeal region; **I:** dorsal surface of the anterior region of the prepharyngeal tube; **F:** prepharyngeal dilator. ***M. clypeobuccalis* (M. 44 / ?/ 0bu1): S:** several paired small bundles; **O:** posterior half of clypeal surface, behind the origin of M. 43; **I:** dorsally on the prepharyngeal tube, behind the insertion of M. 43; **F:** dilator of the posteriormost prepharynx. ***M. frontobuccalis anterior* (M. 45 / ? / 0bu2): S:** a pair of well-developed vertical muscles; **O:** frontal region; **I:** dorsally on the anatomical mouth, directly behind the frontal ganglion, mesad M. 41 / 0hy1; **F:** dilator of the anterior precerebral pharynx. ***M. frontobuccalis posterior* (M. 46 / ? / 0bu3): S:** well-developed, with two subcomponents; M. 46a, closely adjacent with M. 45; **O:** frontal region, very close to the origin of M. 45; **I:** dorsal wall of the anterior pharynx, directly behind the insertion of M. 45; **F:** pharyngeal dilator; M46b, two thin bundles; **O:** posterior frontal region; **I:** medially on the dorsal wall of the anterior pharynx, behind M46a and in front of the brain; **F:** pharyngeal dilator.

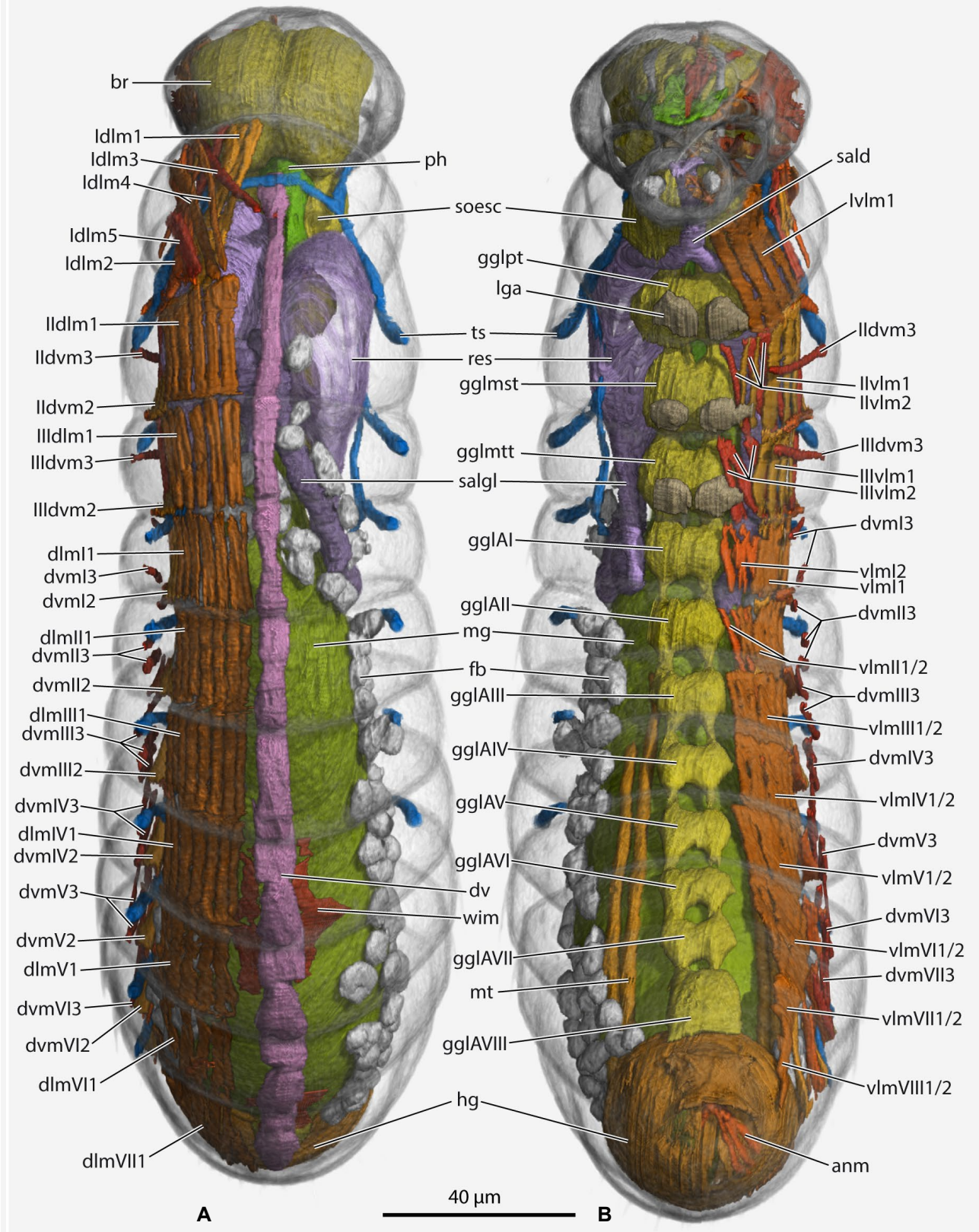

Fig. 10: 3D reconstruction of the 3rd instar larva of *Ooceraea biroi*, dorsal vessel, fat body, postcephalic musculature, salivarium, and digestive, nervous, and tracheal systems. **A:** dorsal view, musculature only shown on the left; **B:** ventral view, musculature only shown on the right. – ***Abbreviations*: anm:** anal muscles; **br:** brain; **dv:** dorsal vessel; **fb:** fat body; **gglpt:** prothoracic ganglion; **gglmst:** mesothoracic ganglion; **gglmtt:** metathoracic ganglion; **gglAI - gglAVIII:** abdominal ganglia I - VIII; **hg:** hindgut; **lga:** leg imaginal discs (leg anlagen); **mg:** midgut; **mt:** Malpighian tubules; **ph:** pharynx; **res:** reservoir; **sald:** salivary duct; **salgl:** salivary gland; **soesc:** suboesophageal complex; **ts:** tracheal system; **wim:** wing muscles; numbering of the muscles as in section Thorax and section Abdomen.

***M. tentoriobuccalis anterior* (M. 48 / M.' 41 / 0bu5): S:** well-developed series of bundles; **O:** anteromedially on the tentorial bridge; **I:** ventral hypopharyngeal wall of prepharynx below bundles of M. 43 and M. 44; **F:** hypopharyngeal retractor and ventral dilator of the prepharynx. ***M. tentoriobuccalis* posterior (M. 50 / M.' 43 / 0bu6): S:** well developed, composed of several bundles; **O:** on the tentorial bridge above M. 48; **I:** ventral wall of the precerebral pharynx; **F:** ventral dilator of the anterior pharynx. ***M. verticopharyngalis* (M. 51 / M.' 37 / 0ph1): S:** thin pair of muscles, atypically extending sideways below and laterad the protocerebral halves; **O:** dorsolaterally near the postoccipital ridge; **I:** laterally on the posterior pharynx, directly below the brain; **F:** dorsal dilator of the posterior pharynx. ***M. tentoriopharyngalis* (M. 52 / M.' 44 / 0ph2): S:** bundles continuous with those of M. 50; **O:** posterolaterally on the posterior tentorial arms; **I:** ventrally on the pharynx below M. 51; **F:** ventral dilator of the posterior pharynx. ***M. pharyngoepipharyngalis* (M. pe / 0pe1): S:** long and unpaired, anteriorly attached to the dorsal prepharynx at the level of 0ci1 and posteriorly on the dorsal pharyngeal surface at the level of M43. ***M. oralis transversalis* (0hy9): S:** transverse muscle of the functional mouth opening, dorsally connecting the lateral edges of the prepharynx in front of the frontal ganglion; **F:** transverse contraction of the oral angles. **Note:** *M. tentoriohypopharyngalis* was not observed by Short (1951) in *Xiphydria*. The muscles 0hy1, 0bu1, 0bu2, and 0bu3 cannot be reliably aligned with Mm.' 35, 36, 38, and 39 of *Xiphydria*, as illustrated by Short (1951).

Cephalic glands. A pair of ovoid glands is present in the anterior premental region (Fig. 6B, D: lbgl). Other glands could not be identified in the head (not visible in µ-CT data).

Cephalic central nervous system and associated structures (Figs. 5, 6). The compact brain is moderately large in relation to the head size; it is located in the posterior half of the head and slightly extended towards the cervical region. Optic lobes and neuropils and antennal nerves are absent. Paired well-developed and straight nerves originating on the anterior protocerebral region enter the labrum and reach its anterior margin. The small frontal ganglion is located above the anatomical mouth and between the anterior parts of the protocerebral hemispheres. The compact suboesophageal ganglion is smaller than the brain and mainly located in the ventral cervical area, anteriorly extending slightly into the posteroventral cephalic region and posteriorly into the prothorax.

Salivarium (Figs. 5, 6, 9). A salivarium as a fold between the hypopharynx and upper prelabial surface is not developed, due to the fusion of the anterior hypopharyngeal part and the dorsal prementum. However, the salivary duct, reservoirs, and the salivary glands are well-developed. The salivary duct is long, Y-shaped, and reaches the anterior wall of the labium anteriorly. The unpaired section divides into the paired branches in the middle region of the prothorax; they turn vertically upward and connect to the large and paired reservoirs on either side of the foregut. The reservoirs are narrow and tubular in the metathoracic region; from there they extend to the base of abdominal segment II, where they are connected to the well-developed salivary glands. The salivary glands are formed by a folded tube on each side and extend forward to the mesothorax. **Musculature of salivarium. *M. hypopharyngosalivaris* (M. 37 / 0hy12): S:** very short, anteroventrally directed; **O:** base of the dorsal wall of the anterior labium; **I:** dorsally on the unpaired salivary duct, close to the opening; **F:** dilator. ***M. praementosalivaris anterior* (M. 38 / 0hy7): S:** oblique, anterodorsally directed; **O:** distal premental region; **I:** ventrolaterally on the unpaired salivary duct, close to the opening; **F:** dilator.

Cervical membrane (Fig. 1): The cervical membrane is almost completely concealed in dorsal view but distinctly exposed laterally and ventrally, widening ventrad, and only slightly shorter than the prothorax in ventral view. Like other unsclerotized areas it displays the rough surface pattern with squamae.

Thorax: Prothorax (Figs. 1, 8, 10). The prothorax is the largest of the three thoracic segments; it is almost as long as the meso- and metathorax combined, and about as long dorsally than on the ventral side. Similar to the other postcephalic segments, it is weakly sclerotized, has a folded surface structure, and lacks defined sclerites. It is composed of three subcomponents: an anteroventral region, which forms a ventral collar enclosing the ventral cervical membrane; a main middle region, which includes the anterior main portion of the pronotal area; and a posterior element with the posterior third of the pronotal region. The three prothoracic subcomponents are separated by deep, nearly vertical folds, the posterior one obliterating dorsally. Notal, pleural, and sternal areas are not delimited. The border between the pro- and mesothorax is distinctly disconnected laterally, with the short dorsal section of the segmental border slightly tilted backwards and ending slightly above half height of the segment; the more distinct ventral section of the border is dorsally continuous with the fold delimiting the posterior prothoracic subsection. Due to this configuration, a broad lateral gap is present between the anterior two thoracic segments. The prothorax lacks spiracles. **Musculature of prothorax. *Dorsal longitudinal muscles*: Idlm1: S:** four paired parallel bundles, directed anteromedially; **O:** paramedially on the posterior margin of the pronotal region; **I:** dorsomedially on the postoccipital region, very close to the border of the postoccipital region and the cervical membrane; **F:** levator of the head. **Idlm2: S:** two paired parallel bundles, directed anterolaterally; **O:** same origin as Idlm1; **I:** laterally on the anterior margin of the cervical membrane, close to the border of the postoccipital region; **F:** rotates the head laterally. **Idlm3: S:** a pair of two oblique, thin bundles, directed anterolaterally; **O:** mesally on the posterior third of the pronotal region; **I:** laterally on the anterior margin of the cervical membrane, mesad Idlm2; **F:** controls lateral movements

of the head. **Idlm4: S:** a pair of two bundles, directed anterolaterally; **O:** paramedially on the posterior margin of the pronotal region, mesad Idlm2; **I:** dorsolaterally on the posterior margin of the cervical membrane; **F:** longitudinal contraction of the prothorax, and control of lateral movements in the cervical region. **Idlm5: S:** two short, paired bundles; **O:** same origin as the medial components of Idlm1 and Idlm2; **I:** anterodorsal end of the disconnected border of the pro- and mesothorax; **F:** controls the degree of curvature of the posterior prothoracic region. ***Ventral longitudinal muscles*: Ivlm1: S:** five paired parallel bundles, longitudinally oriented, slightly converging anteriorly; **O:** paramedially on the posterior margin of the prosternal region; **I:** medially on the tentorium; **F:** retractor and possibly depressor of the head. ***Dorsoventral muscles*: Idvm1: S:** two pairs of oblique bundles; **O:** ventrolaterally on the anterior region of the disconnected border of the pro- and mesothorax, between Ivlm1 and IIdvm1; **I:** dorsolaterally on the postoccipital region, between the insertion of Idlm1 and Idvm2; **F:** levator of the head. **Idvm2: S:** a pair of oblique, thin muscles; **O:** laterally on the middle prosternal region; **I:** dorsolaterally on the posterior margin of the cervical membrane, laterad Idvm1; **F:** possibly levator of the head, controls the degree of curvature of the anterior part of the prothorax. **Idvm3: S:** two oblique, paired, thin bundles; **O:** ventrolaterally on the anterior margin of the cervical membrane; **I:** dorsolaterally on the postoccipital region, laterad Idvm2; **F:** levator, possibly also rotating the head laterad. **Idvm4: S:** a pair of vertical bundles; **O:** ventrolaterally on the anterior margin of the cervical membrane; **I:** laterally on the postoccipital region, laterad Idvm3; **F:** rotates the head laterad.

Meso- and metathorax (Figs. 1, 8, 10). The mesothorax is slightly longer than the metathorax. The border between them is also disconnected, but much less widely than between the pro- and mesothorax. The equally long dorsal and ventral sections of the dividing constriction are slightly interrupted laterally at about half height of this body region; the dorsal section is slightly tilted posteriorly and the ventral section slightly anteriorly. Each segment bears one pair of spiracles, which are situated slightly above the segmental half height as seen in lateral view. **Musculature of meso- and metathorax. *Dorsal longitudinal muscles*: II / IIIdlm1: S:** six pairs of parallel bundles; **ADA** (= anterodorsal attachment)**:** paramedially on the anterior margin of the pronotal / mesonotal region; **PDA** (= posterodorsal attachment)**:** paramedially on the posterior margin of the mesonotal / metanotal region; **F:** longitudinal contraction of the segment. ***Ventral longitudinal muscles*: IIvlm1: S:** five pairs of parallel bundles; **AVA** (= anteroventral attachment)**:** paramedially on the anterior margin of the mesosternal region; **PVA** (= posteroventral attachment)**:** paramedially on the posterior margin of the mesosternal region; **F:** longitudinal contraction of the segment. **IIvlm2: S:** three pairs of parallel bundles, each of them crossing one bundle of IIvlm1; **AVA:** paramedially on the anterior margin of the mesosternal region, each bundle attached slightly mesad the subcomponents of IIvlm1; **PVA:** paramedially on the posterior margin of the mesosternal region, very close to the attachment site of IIvlm1; **F:** longitudinal contraction of the segment, control curvature of the body. **IIIvlm1: S:** four paired parallel bundles; **AVA:** paralaterally on the anterior margin of the metasternal region; **PVA:** paralaterally on the posterior margin of the metasternal region; **F:** longitudinal contraction of the segment. **IIIvlm2: S:** three paired oblique bundles, the lateral one crossing two bundles of IIIvlm1; **AVA:** paramedially on the anterior margin of the metasternal region, three bundles together mesad the attachment of IIIvlm1; **PVA:** paramedially on the posterior margin of the metasternal region, the mesal bundle mesad IIIvlm1 and the lateral two bundles very close to the attachment of IIIvlm1; **F:** longitudinal contraction of the segment and control of body curvature. ***Dorsoventral muscles*: II / IIIdvm1: S:** two paired vertical bundles; **DA** (= dorsal attachment)**:** dorsolaterally on the pro- / mesothoracic and meso- / metathoracic border, between Idlm1 and IIdvm4 / IIdlm1 and IIIdvm4, respectively; **VA** (= ventral attachment)**:** ventrolaterally on the pro- / mesothoracic and meso- / metathoracic border, between Ivlm1 and IIdvm2 / IIvlm1 and IIIdvm2, respectively; **F:** connect tergal and sternal regions, stabilize segments, slight dorsoventral compression. **II / IIIdvm2: S:** a pair of oblique, well-developed muscles; **DA:** dorsolaterally on the border of the meso- and metathorax and metathorax and abdominal segment I, between IIdlm1 and IIIdvm1 / IIIdlm1 and dvmI1, respectively; **VA:** ventrolaterally on the pro- / mesothoracic and meso- / metathoracic border, between IIvlm1 and IIdvm1 / IIIvlm1 and IIIdvm1, respectively; **F:** levator of the ventral part of the preceding segment. **II / IIIdvm3: S:** a pair of thin vertical muscles; **DA:** laterally on the middle region of the mesothorax / metathorax; **VA:** ventrolaterally on the middle region of mesothorax / metathorax; **F:** connect tergal and sternal regions, stabilize segments. **II / IIIdvm4: S:** a pair of oblique, thin muscles; **DA:** dorsolaterally on the pro- / mesothoracic and meso- / metathoracic border, between IIdlm1 and IIdvm1 / IIIdlm1 and IIIdvm1; **VA:** ventrolaterally on the pro- / mesothoracic and meso- / metathoracic border, between IIvlm1 and IIIdvm1 / IIIvlm1 and dvmI1, respectively; **F:** stabilize the connection between the segments.

Leg imaginal discs (Figs. 9, 10). The ovoid leg imaginal discs (anlagen) are located ventrally in the posterior half of each thoracic segment. The prothoracic imaginal discs are slightly larger than those of meso- and metathorax. They are not visible externally.

Abdomen (Figs. 1, 8, 10). The abdomen is composed of ten segments (Fig. 1: AI - AX). It is slightly less than 0.5 mm long. The cuticular surface structure is similar to that of the thoracic segments, but the posterior two segments, AIX and AX, are less distinctly sculptured and the cuticle appears more sclerotized. AI - AIX are almost as long as the metathorax, and AX is only slightly shorter. In dorsal view, AI - AV gradually widen, with AV being

the widest; AVI - AIX narrow progressively; the terminal segment, AX, is conical and much less voluminous than the others. In lateral view, AI - AV gradually increase in height; AVI is approximately as high as AV, and AVII - AIX slope downwards dorsally towards the abdominal apex formed by the tip of AX. Each border between adjacent segments is disconnected, similar to the meso- / metathoracic border. Paired, rounded spiracles are present slightly above half height on the lateral region of AI - AVIII (spiracles AVIII are not visible in the μ-CT scans but easily distinguishable in the SEM images). **Musculature of abdomen.** The segmental abdominal musculature is serially homologous to the meso- and metathoracic muscle systems, and only slightly varies across AI - AVIII. Each segment has a broad group of dorsal longitudinal muscles and two slightly overlapping groups of ventral longitudinal muscles. Vertical and oblique muscles are present in the lateral segmental regions. The ventral longitudinal muscles slightly differ in the number of bundles among AI - AVI and are distinctly reduced in AVII and AVIII. Only a single pair of ventral longitudinal muscles is present in AIX, probably homologous to vlmI1 - VIII1. ***Dorsal longitudinal muscles of segments I - VIII*: dlmI1 - VIII1: S:** a pair of parallel bundles; **ADA:** paramedially on the anterior margin of the dorsal part of abdominal segments I - VIII; **PDA:** paramedially on the posterior margin of the dorsal part of abdominal segments I - VIII; **F:** longitudinal contraction of the segment. ***Ventral longitudinal muscles of segments I - VIII*: vlmI1 - VIII1: S:** a pair of parallel bundles; **AVA:** paramedially on the anterior margin of the ventral region of abdominal segments I - VIII; **PVA:** paramedially on the posterior margin of the ventral region of abdominal segments I - VIII; **F:** longitudinal contraction of the segment. **vlmI2 - VII2: S:** a pair of oblique bundles with parallel arrangement, crossing bundles of vlmI1 - vlmVII1; **AVA:** paramedially on the anterior margin of the ventral part of abdominal segments I - VII, slightly mesad vlmI1 - vlmVII1; **PVA:** the same attachment as vlmI1 - vlmVII1; **F:** longitudinal contraction of the segment and control the curvature of the body. ***Dorsoventral muscles of segments I - VIII*: dvmI1 - VIII1: S:** a pair of thin vertical bundles; **DA:** dorsolaterally on the border of the metathorax and of each of abdominal segments I - VIII; **VA:** ventrolaterally on the border of the metathorax and each of abdominal segments I - VIII; **F:** connect tergal and sternal regions, stabilize segments, and slightly compress them dorsoventrally. **dvmI2 - VIII2: S:** a pair of oblique, well-developed muscles; **DA:** dorsolaterally on the border of each of abdominal segments I - IX; **VA:** ventrolaterally on the border of the metathorax and each of abdominal segments I - VIII; **F:** levator of the ventral part of the preceding segment. **dvmI3 - VIII3: S:** several bundles of thin vertical muscles, located laterad all other abdominal muscles; **DA:** dorsolaterally on abdominal segments I - VIII; **VA:** ventrolaterally on abdominal segments I - VIII; **F:** connect tergal and sternal regions, stabilize segments. ***Ventral longitudinal muscles of segment IX*: vlmIX1: S:** a pair of parallel bundles; **AVA:** paramedially on the anterior margin of the ventral region of abdominal segment IX1; **PVA:** paramedially on the posterior margin of the ventral region of abdominal segment IX1; **F:** longitudinal contraction of the segment. ***Anal muscles of segment X*: S:** a pair of fan-shaped muscles, each pair including four bundles; **O:** paramedially on the anterior margin of the dorsal part of abdominal segment X; **I:** dorsomedially on the anus; **F:** levator of the anal opening.

Postcephalic nervous system (Fig. 9). A pair of separate ganglia is present in each thoracic segment and in abdominal segments I - VII, and a complex in abdominal segment VIII; they are linked by paired connectives, forming the postcephalic ganglionic chain, which is connected to the suboesophageal complex anteriorly and reaches the ventromedian part of the rectum posteriorly. The rectangular terminal ganglionic complex VIII is larger than the individual abdominal ganglionic pairs I - VII.

Postcephalic digestive system (Figs. 8, 9). The postcephalic digestive system consists of a short, tubular esophagus, a long, expanded midgut, and a very short hindgut. The esophageal diameter is almost uniform, but the digestive tract is distinctly widened at the anterior end of the midgut in the border region between the meso- and metathorax. A differentiated crop and proventriculus are not developed. The valvula cardiaca is cylindrical and sheathed by the anterior part of the peritrophic membrane. Caeca and regenerative crypts are absent. The voluminous midgut extends through most of the postcephalic segments; it is divided into two morphologically different sections, a short and relatively narrow anterior portion and a long, swollen posterior part with an enlarged lumen. The anterior portion is only about one sixth as long as the entire midgut, about as long as the valvula cardiaca; the lumen is about half as wide as that of the posterior midgut region. The posterior portion is markedly enlarged and extends to the border between abdominal segments VII and VIII; the midgut is posteriorly closed, its lumen thus not connected with that of the hindgut. The hindgut is attached to the dorsomedial portion of the terminal midgut, and its anterior part is much narrower than the midgut lumen. The Malpighian tubules originate at the midgut-hindgut junction, two on each side; they are straight, elongated, and extend anteriorly to the border between the abdominal segments II and III. A valvula pylorica is not visible. The rectum is markedly enlarged, almost globular, with a diameter approximately equal to that of the posterior part of the midgut, and posteriorly opens at the anus on the apex of abdominal segment X.

Tracheal system (Figs. 9, 10). The tracheal system is well-developed (but only recognizable as disconnected fragments in μ-CT data). Transverse tracheae in the anterior region of the prothorax split into paired subunits laterally, entering into head and postcephalic body, respectively. Paired tracheal stems are present laterad the gut; posteriorly, they can be traced in the μ-CT scan to abdominal segment VII, while spiracles AVIII are visible only on SEM micrographs.

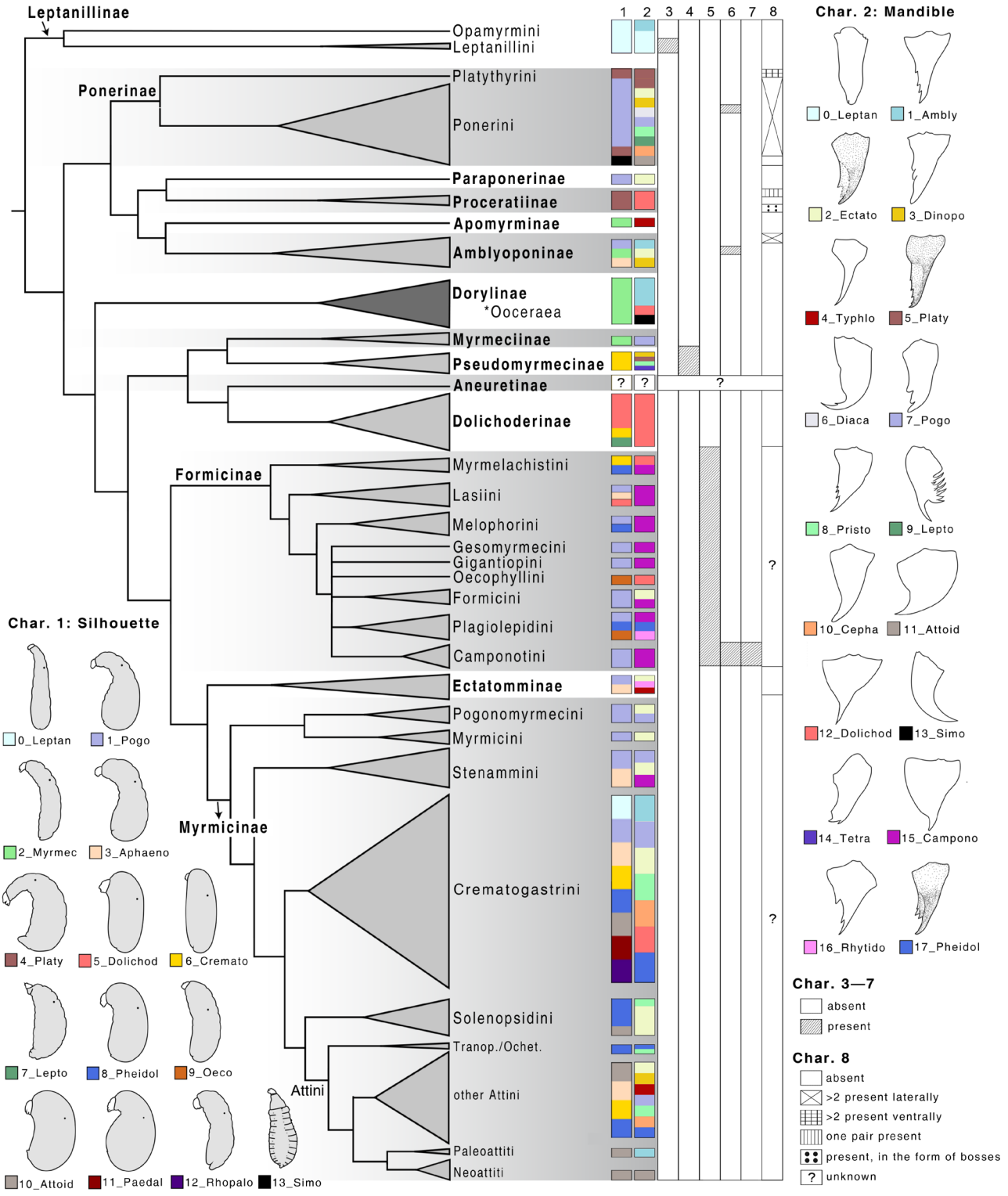

Fig. 11: State mapping onto the simplified topology of Romiguier & al. (2022). Larval silhouettes and mandibles redrawn after Wheeler & Wheeler (1957, 1976, 1986).

Fat body (Figs. 9, 10). The fat body extends through most postcephalic segments, reaching abdominal segment VIII posteriorly. In dorsal view, the distribution of fat body tissue appears Y-shaped, concentrated in the dorsal region in the thorax, and mainly on the lateral sides in the abdomen.

Dorsal vessel (Figs. 9, 10). The dorsal vessel extends from the brain to the middle region of abdominal segment VIII; it is slightly wider in the abdomen than it is in the head and thorax. The wing muscles of the dorsal vessel are recognizable in abdominal segments IV and V.

Ant larval morphological diversity

We summarize the patterns of morphological character distribution across the ant phylogeny, with the states for *Ooceraea* specifically noted in Figure 11. Structures defined in characters 3 - 7 are absent in *Ooceraea*. Characters 1 (larval silhouette) and 2 (larval mandibles) are markedly diverse across ant lineages. A summary of distribution patterns for each character is provided as following:

Character 1. Body form: *Ooceraea* has a "myrmecioid" body form, which is commonly found within Dorylinae, and also occurs in Myrmeciinae and some Amblyoponomorpha (distant terminals only). The larval silhouette of Leptanillinae is "leptanilloid" (*sensu* Wheeler & Wheeler 1957, 1976, 1986), while the "pogonomyrmecoid" silhouette is the most wide-spread one across poneroformicines, with the thorax and first few abdominal segments forming a "neck", and the majority of the abdominal segments forming a bulbous "rump". Among the clade Poneria ("poneroids"), the body form appears "platythyreoid" in Proceratiinae and *Platythyrea*. The Ponerini display further variation, most notably the unique form of *Simopelta* (e.g., Wheeler & Wheeler 1957). Pseudomyrmecinae appear consistently "crematogastroid", with this form also occurring in *Azteca* (Dolichoderinae), *Myrmelachista* (Formicinae), and some groups of Myrmicinae, including the Cephalotina (*Cephalotes*, *Procryptocerus*) and various Crematogastrini (*Cataulacus*, *Crematogaster*, *Temnothorax*, *Xenomyrmex*). Dolichoderinae are characterized by the "dolichoderoid" form, with the exception of *Azteca* (noted above) and *Leptomyrmex*, with the "leptomyrmecoid" body shape. Most larvae of Formicinae are "pogonomyrmecoid", with the exception of *Paratrechina sensu lato* ("dolichoderoid"), *Prenolepis* ("aphaenogastroid"), *Oecophylla* ("oecophylloid"), and various "pheidoloid" groups, including *Brachymyrmex*, *Stigmacros*, *Aphomomyrmex*, and *Petalomyrmex*. Among the sampled Ectatomminae, only *Typhlomyrmex* differed from the pogonomyrmecoid silhouette, having the aphaenogastroid form. The most complex group is Myrmicinae, which displays considerable variation among its vast diversity. Most broadly, the Myrmicini and Pogonomyrmecini retain the pogonomyrmecoid form, while some larvae of Stenammini are aphaenogastroid. The remaining tribes (Attini, Crematogastrini, Solenopsidini), which probably form a clade (Romiguier & al. 2022), display a variety of forms, which we will not summarize here as this should wait until this complex radiation is better resolved.

Character 2. Mandible form: Mandibular morphology exhibits considerable diversity across the subfamilies. The amblyoponoid mandible form is characteristic of most Dorylinae, including *Ooceraea*. Within Leptanillinae, *Opamyrma* has the "amblyoponoid" form, and *Leptanilla* is defined by the "leptanilloid" form, respectively. The mandible forms of Paraponerinae, Proceratiinae, Apomyrminae, Myrmeciinae, and Dolichoderinae are uniform across their members, showing no internal variation. Specifically, Paraponerinae exhibit the "dinoponeroid" form, Proceratiinae and Dolichoderinae have the "simoponoid" form, Apomyrminae are characterized by the platythyreoid form, and Myrmeciinae consistently display the pristomyrmecoid form. Within Formicinae, the "camponotoid" form dominates, though variation exists in specific genera like *Proformica* (ectatommoid form) and *Oecophylla* (dolichoderoid form). This diversity of mandibles across subfamilies illustrates the adaptive morphological responses that might be linked to specific feeding strategies or habitat requirements. Within the Ectatomminae, it appears that *Rhytidoponera* and *Typhlomyrmex* have diverged, with these genera having the "rhytidoponeroid" or "typhlomyrmecoid" forms, respectively. The remaining subfamilies, such as Ponerinae, Amblyoponinae, and Myrmicinae are also variable across their specific members.

Character 3. Leptanilline protuberance: The leptanilline protuberance (a unique ventral prothoracic projection) is unique to *Leptanilla*, lacking in *Opamyrma* and all other ant lineages.

Character 4. Trophothylax: Trophothylax is an autapomorphy of Pseudomyrmecinae.

Character 5. Mandibular ridges: The presence of mandibular ridges is an autapomorphy of Formicinae.

Character 6. Chiloscleres: Chiloscleres mainly occur in Camponotini, although similar structures can be found in *Mystrium* (Amblyoponinae) and *Simopelta* (Ponerini).

Character 7. Praesaepium: The praesaepium is an autapomorphy of Camponotini.

Character 8. Postcephalic tubercles: Tubercles on the body posterad the head mainly occur in Ponerinae, even though with notable variation within this subfamily. For example, *Platythyrea* have ventral tubercles (state 2, unique), whereas lateral tubercles are present in Ponerini (state 1). Proceratiinae exhibit further diversity, with either bosses (i.e., convex projections; state 4) in *Proceratium*, or one pair only (state 3) or none (state 0) in *Discothyrea*.

Discussion

To comprehend the larva of *Ooceraea biroi* it is necessary for us to contextualize our observations at two levels. The first level is phylogenetically broad and based on direct comparative morphology of *Ooceraea* with other Hymenoptera and Holometabola (see section Larval evolution in Hymenoptera and Holometabola), dividing this between cephalic and postcephalic anatomy (see section Larval cephalic morphology and section The postcephalic skeletomuscular system, respectively). The second level is focused on ants themselves (see section The diversity of ant larvae), which is limited to evolutionary patterns of external morphology and the nervous system as these are the only comparative data available to date for the diversity of ant larvae. It will be a major objective of the coming years to link these two levels of comparison. To do so will require replication of the present study for a phylogenetically diverse sample of ant larvae. In order to guide these studies, we point out a number of trends in ant

larval evolution that we infer based on our comparisons in section Patterns of morphological variation across ants. We expect that a program of comprehensive anatomical surveys of ant larvae among species and within species will provide fundamental insights into the role of this stage in the biology of ant colonies and will be its own subject of inquiry.

Larval evolution in Hymenoptera and Holometabola

Evolutionary transformations of immature stages of Holometabola have likely progressed in three main directions: (1) agile and slender campodeid larvae with well-developed legs and often prognathous heads have evolved in Coleopterida and Neuropterida, and also occur in Trichoptera (Rhyacophilidae) and Mecoptera (Nannochoristidae) (e.g., Beutel & al. 2009, 2011, 2019, Friedrich & al. 2015); (2) an intermediate type as in the symphytan grade of Hymenoptera, several groups of Coleoptera (e.g., Scarabaeoidea; Crome 1957), the vast majority of Lepidoptera, and in Mecoptera excl. Nannochoristidae, with a well-developed orthognathous head, relatively short legs, and a moderately or weakly sclerotized postcephalic body, often with leg-like protrusions on abdominal segments (e.g., Mason & Huber 1993); and (3) legless larvae ("maggots"), either with a distinctly developed head like in the coleopteran Curculionidae, in apocritan larvae, and larvae of the dipteran nematoceran grade (e.g., Schneeberg & al. 2012), or with a distinctly or largely reduced head capsule and highly modified cephalic appendages like in Brachycera of Diptera (e.g., Beutel & al. 2011, 2022, Wipfler & al. 2012). Obviously, the larvae of *Ooceraea* and other ants belong to form (3), in this case with a well-developed head capsule.

The larva of *Ooceraea* is of a grub-like form (Fig. 1), simplified and legless as in all other apocritan groups, and also in the ectoparasitic "sawflies" of the family Orussidae (e.g., Vilhelmsen 2003). Larval synapomorphies of a clade Orussidae + Apocrita were outlined by Vilhelmsen (1997, 2003), including reduced number of antennomeres, distinctly reduced maxillary palps, absence of the lateral cervical sclerites, and complete absence of the thoracic legs. The complete reduction of the lateral eyes is a feature shared with the wood-boring larvae of the symphytan Siricidae and related groups (Vilhelmsen 2003). However, reduction or loss of light sensing organs is a common feature of holometabolous larvae with a cryptic life style, as for instance in *Xyela* of the symphytan grade (Beutel & al. 2008), in maggots of the dipteran Tipulidae (Neugart & al. 2009), or in wood-boring coleopteran larvae of Archostemata (Yavorskaya & al. 2015). The legless, grub-like larval form of *Ooceraea* and Apocrita (+ Orussidae) in general is derived from a condition found in the symphytan grade (e.g., Parker 1935, Smith & Middlekauff 1987, Yuasa 1922), likely with an intermediate wood-boring stage leading to ectoparasitism of other wood-boring holometabolan larvae (e.g., Vilhelmsen 1997), and then to parasitism of various groups of arthropods, and eventually to the development of larvae in nests of eusocial adults in the lineages Vespidae, Formicidae, and Apidae.

The condition found in immature stages of symphytan families such as Xyelidae or Tenthredinidae (e.g., Smith & Middlekauff 1987) is close to the groundplan of holometabolan larvae outlined in Peters & al. (2014). This includes a well-developed orthognathous head with somewhat simplified antennae and mouthparts, which is otherwise only slightly modified compared with conditions found in adults, and with a well-developed set of cephalic muscles (Parker 1935, Beutel & al. 2008). The thoracic legs are well-developed in the presumptive holometabolan larval groundplan (e.g., Beutel & al. 2011, Peters & al. 2014). However, the locomotory apparatus is progressively reduced within the symphytan families and entirely absent in the clade Orussidae + Apocrita (Vilhelmsen 1997, 2003). Abdominal prolegs, typically present in larvae of the symphytan grade (Smith & Middlekauff 1987), were likely absent in larvae of the last common ancestor of Holometabola. We suggest that the presence is a derived groundplan feature of the entire Hymenoptera, with secondary loss in wood-associated symphytan groups and in the clade Orussidae + Apocrita. The tergites of the postcephalic segments are simple but usually distinctly developed in most symphytan larvae (Smith & Middlekauff 1987), a condition that was likely also present in a hypothetical ancestral larva of Holometabola. In contrast, pleural elements are more or less restricted to the vicinity of the leg bases, and sternal elements are poorly developed or obsolete in ant larvae and in all other groups of Orussidae + Apocrita (e.g., Beutel & al. 2011, Peters & al. 2014).

Larval cephalic morphology: The cephalic morphology of the head of *Ooceraea* is distinctly simplified as in the groundplan of the clade Orussidae + Apocrita (Vilhelmsen 1997, 2003), with reduced sensorial equipment, notably reduced antennae and missing light sensing organs, and simplified maxillary and labial palps. Despite the simplifications, the relatively well-sclerotized head capsule still bears distinct sets of long setae and also short sensilla (Figs. 2 - 4), similar to much less modified larvae of other holometabolous groups, as for instance Megaloptera (Beutel & Friedrich 2008), Coleoptera (e.g., Crome 1957, Yavorskaya & al. 2015), Trichoptera (Friedrich & al. 2015), or Mecoptera (Beutel & al. 2008). The general head configuration of *Ooceraea* (Fig. 2) is similar to a condition found in larvae of the symphytan grade, which is orthognathous, distinctly sclerotized, and equipped with a free labrum (e.g., Beutel & al. 2008, Parker 1935, Smith & Middlekauff 1987, Yuasa 1922). However, the labrum is retractable in symphytan larvae, *Xyela* for instance (Beutel & al. 2008), but not in *Ooceraea*, where extrinsic muscles are missing. The antennae of symphytan larvae are more or less short but usually well-developed and composed of up to seven segments (Beutel & al. 2008, Smith & Middlekauff 1987), whereas they are absent in *Ooceraea* and other groups of the Orussidae + Apocrita clade (Tab. 1; Vilhelmsen 1997, 2003). The mandibles

Tab. 1: Comparisons of larval cephalic muscles. *Oobi-L* = *Ooceraea biroi* larva; *Apme*-L = *Apis mellifera* larva (Nelson, 1924); *Xy*-L = *Xyela* sp. larva (Beutel & al. 2008); *Foru-A* = *Formica rufa* adult (Richter & al. 2020). Uncertain conditions are indicated with question marks.

Muscles of head	***Oobi-L***	***Apme-L***	***Xy*-L**	***Foru-A***
Antenna				
M. tentorioscapalis anterior	–	–	M1	M1 / 0an1
M. tentorioscapalis posterior	–	–	M2	M2 / 0an2
M. tentorioscapalis lateralis	–	–	M3	M3 / 0an3
M. tentorioscapalis medialis	–	–	M4	M4 / 0an4
M. scapopedicellaris lateralis	–	–	–	M5 / 0an5
M. scapopedicellaris medialis	–	–	–	M6 / 0an6
Labrum				
M. labroepipharyngalis	M7 / 0lb5	?	M7	–
M. frontolabralis	–	RLm	M8	–
M. frontoepipharyngalis	–	ClpMcl	M9	M9 / 0lb2
Mandible				
M. craniomandibularis internus	M11 / 0md1	EMd	M11	M11 / 0md1
M. craniomandibularis externus	M12 / 0md3	RMd	M12	M12 / 0md3
M. tentoriomandibularis	–	–	M13	M13 / 0md8
Maxilla				
M. craniocardinalis	–	–	–	M15 / 0mx1
M. tentoriocardinalis	M17 / 0mx3	EMx?	M17	M17 / 0mx3
M. tentoriostipitalis anterior	M18 / 0mx4	EMx	M18	M18 / 0mx4
M. craniolacinialis	M19 / 0mx2	RMx	M19	–
M. stipitolacinialis	–	–	M. stipitolacinialis	M20 / 0mx6
M. stipitogalealis	–	–	–	M21 / 0mx7
M. stipitopalpalis externus	–	–	–	M22 / 0mx8
M. palpopalpalis maxillae	–	–	–	M24 - 27 / 0mx12 - 15
Labium				
M. submentopraementalis	M28 / 0la8	–	M28	–
M. tentoriopraementalis inferior	M29 / 0la5	–	M29	M29 / 0la5
M. tentoriopraementalis superior	M30 / 0la6	1RLb	M30	–
M. praementoparaglossalis	–	–	–	M31 / 0la11
M. praementoglossalis	–	–	–	M32 / 0la12
M. praementopalpalis internus	–	–	M33	–
M. praementopalpalis externus	–	–	M34	M34 / 0la14
M. palpopalpalis labii	–	–	–	M35, 36 / 0la16, 17
Digestive tract				
M. frontohypopharyngealis	M41 / 0hy1	SDilPhy	M41	M41 / 0hy1
M. tentoriohypopharyngalis	–	–	M42	M42 / 0hy3
M. clypeopalatalis	M43 / 0ci1	LevEphy	M43	M43 / 0ci1
M. clypeobuccalis	M44 / 0bu1	LevEphy	M43?	M44 / 0bu1
M. frontobuccalis anterior	M45 / 0bu2	LevPhy	M45	M45 / 0bu2
M. frontobuccalis posterior	M46 / 0bu3	?	M46	M46 / 0bu3
M. tentoriooralis	–	–	–	M47/ 0hy2
M. tentoriobuccalis anterior	M48 / 0bu5	DilPhy	M48	M48 / 0bu5
M. tentoriobuccalis posterior	M50 / 0bu6	DilPhy	M50	M50 / 0bu6

Muscles of head	*Oobi-L*	*Apme-L*	*Xy*-L	*Foru-A*
M. verticopharyngalis	M51 / 0ph1	?	M51	–
M. tentoriopharyngalis	M52 / 0ph2	?	M52	M52 / 0ph2
M. pharyngoepipharyngalis	Mpe / 0pe1	–	lm	Mpe
M. oralis transversalis	0hy9	–	transverse muscles	M67 / 0hy9
M. annularis stomadaei	–	–	–	M68 / 0st1
M. longitudinalis stomadaei	–	–	–	M69 / 0st2
Salivarium				
M. hypopharyngosalivaris	M37 / 0hy12	–	–	M37 / 0hy12
M. praementosalivaris anterior	M38 / 0hy7	2RLb	–	M38 / 0hy7
M. prementosalivaris posterior	–	–	–	M39 / 0hy7

are much more massive in larvae of *Xyela* (BEUTEL & al. 2008) and larvae of other symphytan groups (e.g., PARKER 1935), apparently suitable for intensive mechanical processing of more or less solid food, even though a grinding mola is always absent (BEUTEL & al. 2008).

The head of larval *Ooceraea* is also similar to the larval head of the mecopteran *Caurinus*, which also has a grub-like body with strongly reduced but still present legs (FABIAN & al. 2015: figs. 1A, 3A). In both cases, the head capsule is well defined, equipped with a well-developed free labrum, functional mandibles, and small, simplified maxillary palps and labium. However, in contrast to *Ooceraea*, the antennae are greatly shortened but still present as two segments in the free-living larvae of *Caurinus*. Additionally, whereas the labium appears large and even bloated in *Ooceraea*, it is greatly reduced in *Caurinus*, scarcely visible between the maxillae. Furthermore, eyes are present in *Caurinus*, with distinctly separated stemmata, in contrast to the eyeless larvae of *Ooceraea*, as well as to the fairly large single lateral eyes in symphytan larvae and larvae of the pistilliferan groups of Mecoptera (BEUTEL & al. 2009, 2011, FABIAN & al. 2015).

The cephalic muscular apparatus of *Ooceraea* (Figs. 3, 4) is only moderately simplified, with a total of 20 intrinsic head muscles excluding two modified muscles (Tab. 1: 0pe1 and 0hy9) of the digestive tract. In comparison, 27 cephalic muscles are found in the larvae of *Xyela* (Hymenoptera), 27 in the slender larvae of Nannochorista (Mecoptera), and 34 in the large larvae of *Neohermes* (Megaloptera) (Tab. 1; BEUTEL & FRIEDRICH 2008, BEUTEL & al. 2008, 2009). The extrinsic labral and all antennal muscles are missing in *Ooceraea*, with additional differences in muscles of the mouthparts and alimentary canal between larval and adult ants (Tab. 1). While the small mandibular 0md8 muscle may be difficult to find in the minute larva, internal muscles of labium and maxilla are clearly missing. Missing in our interpretation are also the extrinsic crandiocardinal muscle (0mx1) and tentoriohypopharyngeal muscle (0hy3), important movers of the maxillolabial complex in adult ants. Instead, larvae have a craniolacinial (0mx2), a submentopremental (0la8), and a lower tentoriopremental muscle (0la6) according to our interpretation here, none of which have been found in adult ants so far. This underlies the rearrangement of the mouthparts during metamorphosis and indicates differences in mouthpart use, which may be an interesting point of future comparison given the different dietary roles of ant larvae in the colony. The muscles of the cibarium and pharynx, including the salivarial muscles which are totally absent in *Xyela*, are very well-developed (with the exception of the absent frontooral muscle 0hy2), enabling the larvae to efficiently imbibe food that is more or less liquid.

Like larvae of the honey bee (WINSTON 1991), ant larvae are essentially feeding machines designed for rapid growth, with a well-developed digestive tract but with more or less reduced structures not relevant for the postembryonic development in the nest. It is apparently a general pattern in Holometabola that muscles of antennae and mouthparts become simplified or reduced along with simplifications of these appendages, although this pattern is not entirely followed by *Ooceraea*, switching some mouthpart muscles out for others, rather than only reducing muscles. That muscles of the digestive tract are always maintained or even increased in complexity may be reflected by the unexpected observation of the presence of M. verticopharyngalis (M. 51) in larvae of *Ooceraea* (Fig. 6). It is noteworthy that absence of this muscle was suggested as an apomorphy of the entire Formicidae as it has never been found in ant adults but is usually present in adults of Aculeata, as well as in symphytan groups such as adults of *Macroxyela* (BEUTEL & VILHELMSEN 2007, RICHTER & al. 2020, ZIMMERMANN & VILHEIMSEN 2016). While the large relative size and position of the brain was suggested as possible explanation for the absence of this muscle in adults (e.g., RICHTER & al. 2020), presence in the larva of *Oocerea* calls this into question to some degree. Although size of the brain is considerable, nearly filling out the posterior lumen of the head, a distinct pair of thin muscles is still found in this region (Fig. 6), albeit in a modified position. In any case, reduction of this muscle is very common in larvae and adults of insects. It is possible that the presence in adults is indeed an autapomorphy of the family, whereas it may have been retained in the larval groundplan or derived secondarily. Further anatomical study of larval head anatomy across the Formicidae is necessary to resolve this question and will certainly yield

new discoveries of diagnostic, functional, and evolutionary significance.

The postcephalic skeletomuscular system: The postcephalic skeleton of larval *Ooceraea* (Fig. 1), Orussidae, and other apocritan groups (Vilhelmsen & al. 2003) is strongly simplified compared with larvae of other holometabolan groups and also compared with winged adult insects (e.g., Friedrich & Beutel 2008, 2010), especially in the thorax. Structures associated with the flight apparatus are completely missing in all holometabolous larvae for obvious reasons. Not only the pronotum is a simple plate, serving for instance as attachment area for neck muscles, but also the tergites of the meso- and metathorax. Additional simplifications, for instance the absence of clearly defined pleural sclerotizations, are obviously related to the loss of legs in larvae of Orussidae and Apocrita, including ants (Vilhelmsen 2003). As is the case for other holometabolan larvae, the segments of the thorax and the abdominal segments are also simple in *Ooceraea*. The absence of a developed male or female genital apparatus makes skeletal and muscular differentiations in the posterior segments superfluous in most groups of Holometabola. Specialized terminal segments occur in some holometabolan groups as for instance in Nannochoristidae (Fraulob & al. 2012), in this case related to specialized breathing organs.

The muscular pattern of the postcephalic body of *Ooceraea* is a regular, homogenous three-dimensional meshwork of dorsal and ventral longitudinal groups of muscles, and vertical and oblique dorsoventral bundles (Figs. 8, 10). Data on the musculature of ant larvae are extremely scarce. However, a very similar condition was described for 4th instar larvae of *Solenopsis* (Myrmicinae) (Petralia & Vinson 1980). Together with the relatively thin postcephalic cuticle, the muscles of the thorax and abdomen form a counterweight to the internal hemolymph pressure, the entire configuration thus technically functioning as a pneu (e.g., Gutmann 1985). This condition superficially resembles a "Hautmuskelschlauch" of worm-like groups outside of Arthropoda, but ring muscles are generally absent in insect larvae (e.g., Hoyle & Williams 1980, Wipfler & al. 2012, Yavorskaya & al. 2015). Somewhat similar conditions also occur in arthropod lineages outside of insects, such as in Onychophora (Hoyle & Williams 1980) or Geophilomorpha (Chilopoda) (Füller 1963), in the former case arguably as a plesiomorphy and arthropod groundplan condition, in the latter case as an apomorphy, correlated with a strongly elongated and multisegmented postcephalic body with very short legs. A similar pattern of postcephalic muscles is also found in *Drosophila* and other brachyceran larvae (Wipfler & al. 2012), with well-developed dorsal and ventral longitudinal bundles and dorsoventral muscles. However, the presence of longitudinal muscles extending over several segments in *Drosophila* (Wipfler & al. 2012) is certainly atypical and a derived condition among holometabolous larvae including *Ooceraea* (e.g., Yavorskaya & al. 2015, Jandausch & al. 2018).

The thoracic musculature is greatly simplified (Figs. 8, 10), very similar to the pattern of the abdominal segments. A partial exception is the prothorax, where dorsal, ventral, and oblique cervical muscles ensure the movability of the head. Similar sets of well-developed neck muscles are almost generally present in holometabolous larvae (e.g., Yavorskaya & al. 2015, Jandausch & al. 2018), with the obvious exception of the maggots of Brachycera (Wipfler & al. 2012). The condition in these dipteran larvae is highly modified, not only in correlation with the largely reduced head capsule, but also with the presence of a newly formed complex cephaloskeleton (Wipfler & al. 2012). The mesothorax of *Ooceraea* comprises a total of seven muscles, a single group of dorsal longitudinal bundles, two units of ventral longitudinal bundles, and four dorsoventral bundles (Fig. 8). In contrast, 23 muscles are present in the same segment of the agile primary larvae of *Mantispa*, excluding intrinsic leg muscles, two dorsal longitudinal muscles, two ventral longitudinal muscles, one dorsoventral muscle, 12 lateral muscles, and six extrinsic leg muscles (Jandausch & al. 2018: fig. 14).

Whereas muscles of the head of *Ooceraea* can be easily associated with their adult equivalents based on defined sites of origin and especially insertion, a homologization with a thoracic neopteran ancestral pattern outlined by Friedrich & Beutel (2008) and Beutel & al. (2014) is only partially possible. It is very likely that the dorsal and ventral longitudinal muscles, by far the largest bundles in the thorax of *Ooceraea* and *Solenopsis* (Petralia & Vinson 1980), are homologous with their equivalents in adult insects of hemimetabolous or holometabolous groups. However, in holometabolous larvae (e.g., Yavorskaya & al. 2015, Jandausch & al. 2018), the areas of origin, that is, dorsal phragmata and ventral furcae and spinae, are less developed (e.g., Jandausch & al. 2018: fig. 14) or absent like in *Ooceraea* (Figs. 8, 10). This is correlated with the missing flight function in the case of the dorsal muscle attachment areas. In contrast to the longitudinal muscles, a homologization of the vertical and oblique dorsoventral thoracic bundles is obviously not possible as the largely undifferentiated exoskeleton lacks clearly defined attachment sites, defined tergal areas, axillary sclerites, defined pleural sclerites, and elements of the legs, especially the coxa and trochanter. In *Drosophila*, the larval muscle system is largely or completely degraded in the early pupal stage, with adult muscles formed de novo during the complete metamorphosis (Schulman & al. 2015). Presently, a documentation of developmental transformations in the pupal stages in Formicidae is not available. However, it appears likely that a similar developmental pattern occurs in ants. Information on the metamorphosis in the postcephalic body of Neuroptera is presently not available. However, the presence of a complex set of lateral muscles and leg muscles suggests that transformations take place instead of a complete replacement.

The diversity of ant larvae

In a parallel to Diptera, where the larvae of the nematoceran grade are morphologically diverse relative to the simplified maggots of Brachycera (e.g., Hennig 1973, Neu-

gart & al. 2009, Schneeberg & al. 2012, Wipfler & al. 2012), the larvae of the symphytan grade are superficially more diverse relative to those of the Apocrita (Smith & Middlekauff 1987). Their structurally simplified body has earned these larvae the unwarranted reputation of appearing generally uniform, to the level of being "nearly featureless" (Mason & Huber 1993). At a very gross scale, the comparison of *Ooceraea* (Dorylinae) and *Solenopsis* (Myrmicinae) larvae (Petralia & Vinson 1980) may support the perception of apocritan larvae, including ants, as simple and sausage- or barrel-shaped lifeforms (Wheeler & Wheeler 1986: fig. 1). This conclusion is not justified, however, when the structural diversity of larvae is considered across the phylogeny of ants. Wheeler & Wheeler (1972, 1976, 1986) have already demonstrated remarkable morphological variation, especially but not only in body shape (Wheeler & Wheeler 1986: fig. 3), while we show here that the individual ant larva is highly complex and rich in structural detail internally. It will be an important goal of future study to determine larva-specific character systems of the internal anatomy as this may provide insights into the evolutionary and possible physiological patterns of this critical life stage.

Framework 1: Patterns of morphological variation across ants: As outlined in the Introduction, the primary framework for understanding the morphological variation across ants is the Wheeler and Wheeler system. In order to place *Ooceraea biroi* in the context of all Formicidae, we evaluated the completeness of character information from the oeuvre of Wheeler and Wheeler (especially Wheeler & Wheeler 1957, 1976, 1986), finding that eight characters could be scored across the family with reasonable completeness. By plotting these at the level of terminals given the recent genomic phylogeny of Romiguier & al. (2022), we are able to observe patterns of overall diversity and of putative particular adaptations. For example, the Formicinae are characterized by mandibular ridges across the whole subfamily (Character 5, state 1), while the Camponotini are defined by occurrence of both chiloscleres and praesaepium (state 1 of Characters 6 and 7). The Camponotini are one of the hyperdiverse lineages of Formicidae, representing 60% of the species-level diversity of their subfamily (Bolton 2024). Moreover, they are characterized by a major evolutionary transition, the obligate trophic endosymbiosis with the bacterium *Blochmannia*, which even plays a role in the developmental patterning of its host (Rafiqi & al. 2020). Are these derivations of larval morphology present in Camponotini related to this major transition, and if so, how? If not, what role do the chiloscleres and praesaepium play in the trophic biology of individual larvae and of larvae in the context of the colony?

Adaptation in larval feeding ecomorphology is also likely indicated by variation in the mandibles, for which numerous forms have been classified by Wheeler & Wheeler (1957, 1976, 1986). The larvae are fed by adults, and in strictly predatory lineages (e.g., Leptanillomorpha, many lineages of the "poneroid clade"), it is possible that variation of larval mandibles is correlated with the prey provided by workers. Among the major groups (Leptanillomorpha, the "poneroid clade", Dorylinae, the "formicoid clade" excluding Dorylinae), the mandible shapes of larvae range from a subtriangular form with one to a few medial teeth to more specialized morphologies with ("ectatommoid") or without ("amblyoponoid") a medial blade (Fig. 11). In contrast, larval *Leptanilla* have shredding mandibles ("leptanilloid") with numerous teeth (Barandica & al. 1994), while the predatory poneroids expanded in larval mandible morphospace, with 12 discrete forms recognized by Wheeler & Wheeler (1957, 1976, 1986). How these mandibles vary functionally and whether they correspond to prey choice, patterns of prey processing, or other variables is yet another open question.

Larval mandibles are somewhat more stable in their patterns of variation among the Doryloformicia, with most sampled Dorylinae having the "amblyoponoid" form, the Dolichoderinae, Myrmeciinae, and Formicinae being defined by their own (nearly) unique forms ("dolichoderoid", "pogonomyrmecoid", "camponotoid"), each with some further variation to explore. However, the Myrmicinae are so diverse in mandibular form that they defy simple summary. Notably, however, molecular phylogenetics in conjunction with our analyses have revealed one tractable action point for experimental study. Although it has been thought that the Attina, that is, the fungus farming ants, have been defined by the "attoid" form, it turns out that the two major clades therein have their own clade-specific forms, with the Paleoattina being "amblyoponoid" and the Neoattina being "attoid". It is possible that these patterns relate to functionally different means of processing fungal or yeast symbionts by the larvae of these evolutionarily interesting and ecologically important ants.

Perhaps the most familiar larval character to field and lab myrmecologists is the body silhouette, which displays remarkable diversity across taxa. The thin "necked" and plump "rumped" "pogonomyrmecoid" form, for example, is a dominant shape of Poneroformicines. However, transitions from this form appear in various other groups, with some members of clade Poneria ("poneroids") independently exhibiting the "platythyreoid" form, the Dorylinae (including *Ooceraea*) and various other groups present as the "myrmecioid" form, and other patterns of repeated shape evolution. Numerous unique shapes have evolved in various taxa, including the bizarre larval form of the ponerine *Simopelta* and the strange double-chin form of *Leptomyrmex*, among others. Recently, Matte & Leboeuf (2024) simplified the Wheeler system to focus on the occurrence of thoracic narrowing or necking, which they find to be correlated with larval activeness and degree of queen-worker dimorphism.

In addition to these patterns, larval simplification is a clear trend in the Formicidae, suggesting that other (internal) structures of the larvae of ants may also undergo unique patterns of derivation. Where reduction of larval segmentation and formation of an egg-like silhouette has evolved, which is numerous times across the

"formicoid clade", what is the functional and fine structural correlation? Are there coordinated patterns of digestive tract modification? Relative investment in fat bodies? Changes in relative growth of the imaginal disks? These questions are only the beginning of anatomical "larvology" for ants. Given that larvae are the necessary intermediates in the collective diet of most ant colonies, there is much work to do to understand the role of these seemingly passive juveniles. To the present day, the functional diversity of larval body processes (tubercles) in the Ponerinae is unknown, and the evolutionary novelties of the leptanilline protuberance of *Leptanilla* and trophothylaces of Pseudomyrmecinae remain mysterious.

One more conclusion from examining the diversity of larval body and mandible shape is the limitation of the terminology of Wheeler and Wheeler when all ants are considered. While larval body shape names were originally defined based on the specific taxa that they occurred in, subsequent study kept revealing more and more independent derivation of some of these body forms. This recurring appearance of similar forms in unrelated taxa introduces considerable confusion and reduces the clarity of the terms of Wheeler and Wheeler as these categories do not necessarily convey evolutionary or functional relationships. While it would be ideal to derive taxon-independent terminology for larval shapes, this may be disruptive given the at this point deep establishment of the terms of Wheeler and Wheeler in the ant literature. If attempted at all, this should also likely be based on a statistical evaluation of larval shapes, using methods such as geometric morphometrics and statistical clustering, to substantiate the appearance-based discretization of different larval forms. The simplification provided by Matte & Lebouf (2024), for example, allowed them to focus on functional traits for phylogenetic and macroevolutionary analysis.

In our analyses, we did not examine patterns in the variation of antennae and hairs due to the paucity of information for the former, and the incredible variation of the latter. Wheeler & Wheeler (1976: fig. 16) observed that the antennae may be lobose, subcylindrical, or knob-shaped, with particular (and unexplained) variation among Ponerinae. Usually, the larval antenna is present as discoids with three spinules each. We observed this condition in *Ooceraea*, despite the fact that only two spinules are present in other known army ant genera of the subfamily Dorylinae, including *Aenictus*, *Dorylus*, *Eciton*, *Labidus*, and *Neivamyrmex* (Wheeler & Wheeler 1976, 1986). The functional significance of this remains unknown. With respect to setae, a dense pattern of medium-length flexible setae and very densely arranged irregular scale-like cuticular structures is present on the surface of the postcephalic body of *Ooceraea* (Fig. 1). In contrast, a very dense and largely homogenous vestiture of short setae is present in *Cerapachys* and *Myrmecia* (Wheeler & Wheeler 1976: p. 47). A similar pattern is developed in *Leptanilla revelierei*, however with the addition of conspicuous long and robust setae, especially concentrated on the abdominal apex. This is arguably a defensive mechanism, similar to conspicuous bundles of robust setae on the abdominal apex of larvae of the beetle family Dermestidae.

Framework 2: Structural conservation in larvae: Because of the scattered nature of taxon and organ system information from studies conducted in the second framework of larval morphology, these studies are best used to evaluate conservation of larval structures.

Perhaps most interesting to note is the apparent conservation of the larval nervous system in relationship to adult ants. Between the larvae of *Ooceraea* and *Solenopsis* (Petralia & Vinson 1980), we observe that the nervous systems are similar, with a brain that is large in relation to the head lumen but lacking optic lobes, a moderately sized suboesophageal ganglion in the ventral postoccipital region, plus seven separate ganglia in the postcephalic body, followed by a slightly enlarged ganglionic complex of abdominal segment VIII. Differing from adult ants and other Hymenoptera (e.g., Richter & al. 2020, 2022), however, the suboesophageal complex of these ant larvae is widely separated from the brain, composed of proto-, deuto-, and tritocerebrum. In clear contrast, in adults, the brain and suboesophageal complex form a compact unit, such that the digestive tract passes through a narrow neural foramen. On the one hand, this difference between stages is remarkable as the loose organization is more similar to the adults of other orders of insects, such as Orthoptera (Snodgrass 1935), indicating that the compact organization is a derived condition with an unknown phylogenetic origin (Xyelidae have an apparent intermediate condition; Beutel & Vilhelmsen 2007). On the other hand, the narrow diameter of the neural foramen in adult ants forms one of several barriers to the consumption of solid food pieces. Another notable barrier in adult ants is formed by the narrow occipital foramen (foramen magnum), which is a derived condition of Formicidae. Additionally, the constriction of the waist in ants and other Apocrita (the diagnostic "wasp waist") poses a further challenge to process solid food particles. The implications of these restrictions on adult diet have, to our knowledge, not been explored.

Other observations are also worth noting, but with as yet unclear evolutionary implications. The tracheal system appears conserved, with spiracles on the meso- and metathorax and abdominal segments I - VIII, as in the vast majority of insects. In larvae of *Ooceraea*, *Solenopsis* (Petralia & Vinson 1980), and *Eciton* (Lappano 1958), the postcephalic digestive tract comprises a simple tube-shaped oesophagus, a very voluminous midgut extending over more than half of the length of the body, and a short hindgut mostly formed by a conspicuous, globular rectum. Strongly developed, Y-shaped salivary ducts are present, opening on the anterior labium. The importance of these glands in social insects was already recognized by Wheeler (1910). Four well-developed Malpighian tubules are present in *Ooceraea*, *Solenopsis* (Petralia & Vinson 1980), and *Eciton* (Lappano 1958). They reach the anterior border of abdominal segment III anteriorly in

Ooceraea, but almost the neck region in the stouter larva of *Solenopsis* (Petralia & Vinson 1980). The fat body is probably generally strongly developed in ant larvae, filling out most of the space between the gut and the layer of muscles and body wall (Fig. 9). A well-developed heart and dorsal aorta are present in both *Solenopsis* and *Ooceraea* larvae. In contrast to larvae of *Eciton* (Lappano 1958), the larval heart is posteriorly closed in *Solenopsis* like in *Apis* (Petralia & Vinson 1980). This is likely also the case in *Ooceraea* (Fig. 9), even though our µ-CT data set did not reveal this condition unambiguously.

Conclusion

In the present study, we provide the first three-dimensional anatomical atlas of the larva of an ant species, documenting all hard and soft tissues that were detectable given the limitations of resolution and contrast for our SR-µ-CT dataset. Through comparison with larvae of other groups of Hymenoptera and Holometabola, we observe that the larva of *Ooceraea biroi* belongs to a distinctly simplified legless form, with a distinct pattern of prothoracic muscles but otherwise with a rather homogenous meshwork of postcephalic muscles. The head capsule is well-developed and retains many cephalic muscles but also has strongly reduced cephalic appendages and sense organs. Integrating over the limited available anatomical studies on other ant larvae, it is likely that these main characteristics are shared across the family. Although an adult anatomy of *O. biroi* is not yet available, we find through comparison with the adult head of *Formica rufa* that it is primarily the muscles of the upper digestive tract that are conserved between these life stages. Among these, the presence of pharyngeal muscles (M. verticopharyngalis) in the larva of *O. biroi*, which are absent in adults of Formicidae, challenges assumptions about their evolutionary loss and suggests they may represent either a retained element of the ant larval groundplan or a secondary derivation specific to larval development. We also observe that the larvae of *O. biroi* and *Xyela* share muscles of the maxillolabial complex that are in the groundplan of the Neoptera but absent in the adults of ants. Through comparison of *O. biroi* in the first framework of larval morphology, we find that this species is similar to other Dorylinae, and we discuss broader patterns of variation arising from our plotting of characters derived from the system of Wheeler and Wheeler. Finally, by comparing the larva of *O. biroi* with those few other ant species for which comprehensive internal anatomical information is available, we find several patterns of conservation of organ systems. The conservation of the cephalic nervous system among *O. biroi* and *Solenopsis invicta* relative to adult ants and other Hymenoptera, however, reveals that the brain and suboesophageal ganglion of adults are much more compactly organized, resulting in the one of several barriers to the consumption of solid food. The evolutionary origin is unknown for this derived, constricted condition of the neural foramen in adult Hymenoptera. Overall, our work demonstrates that certain technical hurdles for the study of larvae and other small and soft-bodied insects can be overcome through the application of µ-CT, which should ideally be complemented by other techniques such as SEM. It is our hope that the larval anatomy provided here will spur further interest in this often overlooked but essential developmental stage of ants.

Acknowledgements

We thank Jill Oberski for copious discussion during the writing process. We are grateful to Beny Wipfler for sharing the *Drosophila* muscle development book with us. DL was supported by China Scholarship Council (2021 - 2022). BEB was supported by research fellowships from the Alexander von Humboldt Stiftung (2020 - 2022) and the Smithsonian Institute National Museum of Natural History (2023). AR was supported by a doctoral scholarship from the Evangelisches Studienwerk Villigst and by the Japan Society for the Promotion of Science (JSPS) as an international postdoctoral research fellow. We acknowledge the KIT light source for provision of instruments at their beamlines and we would like to thank the Institute for Beam Physics and Technology (IBPT) for the operation of the storage ring, the Karlsruhe Research Accelerator (KARA). We thank Angelica Cecilia and Marcus Zuber for their support during beamtime. DJCK is an investigator of the Howard Hughes Medical Institute. This is Clonal Raider Ant Project paper number 35.

Declaration on use of generative artificial intelligence tools

The authors declare that they did not utilize generative artificial intelligence tools in any part of the composition of this manuscript.

Author contributions

Conceptualization: DL, BEB, AR, RGB. Methodology: DL, BEB, AR, LOC, TvdK, RGB. Formal analysis: DL, BEB, AR, TvdK, RGB. Investigation: DL, BEB, AR, RGB. Resources: TvdK, DJCK, RGB. Data curation: DL, BEB, TvdK. Writing, original draft: DL, BEB, AR, RGB. Writing, review & editing: DJCK. Visualization:DL, BEB, RGB. Funding acquisition: BEB, AR, TvdK, DJCK.

Conflict of interest

The authors declare no competing interest.

References

Adams, R.M., Larsen, R.S., Stylianidi, N., Cheung, D., Qiu, B., Murray, S.K., Zhang, G. & Boomsma, J.J. 2021: Hairs distinguish castes and sexes: identifying the early ontogenetic building blocks of a fungus-farming superorganism (Hymenoptera: Formicidae). – Myrmecological News 31: 201-216.

Athias-henriot, C. 1947: Recherches sur les larves de quelques fourmis d'Algérie. – Bulletin Biologique de la France et de la Belgique 81: 247-272.

Barandica, J.M., López, F., Martínez, M.D. & Ortuño, V.M. 1994: The larvae of *Leptanilla charonea* and *Leptanilla zaballosi* (Hymenoptera, Formicidae). – Deutsche Entomologische Zeitschrift 41: 147-153.

Berlese, A. 1902: Osservazioni su fenomeni che avvegono durante la ninfosi degli insetti metabolici. – Rivista di Patologia Vegetale 9: 177-344.

Beutel, R.G. & Friedrich, F. 2008: Comparative study of larval head structures of Megaloptera (Hexapoda). – European Journal of Entomology 105: 917-938.

Beutel, R.G., Friedrich, F. & Economo, E.P. 2022: Patterns of morphological simplification and innovation in the megadiverse Holometabola (Insecta). – Cladistics 38: 227-245.

Beutel, R.G., Friedrich, F., Hörnschemeyer, T., Pohl, H., Hünefeld, F., Beckmann, F., Meier, R., Misof, B., Whiting, M.F. & Vilhelmsen, L. 2011: Morphological and molecular evidence converge upon a robust phylogeny of the megadiverse Holometabola. – Cladistics 27: 341-355.

Beutel, R.G., Friedrich, F., Yang, X.K. & Ge, S.Q. 2014: Insect morphology and phylogeny: a textbook for students of entomology. – Walter de Gruyter, Berlin, pp. 24-28.

Beutel, R.G., Kristensen, N.P. & Pohl, H. 2009: Resolving insect phylogeny: the significance of cephalic structures of the Nannomecoptera in understanding endopterygote relationships. – Arthropod Structure & Development 38: 427-460.

Beutel, R.G., Krogmann, L. & Vilhelmsen, L. 2008: The larval head morphology of *Xyela* sp. (Xyelidae, Hymenoptera) and its phylogenetic implications. – Journal of Zoological Systematics and Evolutionary Research 46: 118-132.

Beutel, R.G., Pohl, H., Yan, E.V., Anton, E., Liu, S.P., Ślipiński, A., Mckenna, D. & Friedrich, F. 2019: The phylogeny of Coleopterida (Hexapoda) – morphological characters and molecular phylogenies. – Systematic Entomology 44: 75-102.

Beutel, R.G. & Vilhelmsen, L. 2007: Head anatomy of Xyelidae (Hexapoda: Hymenoptera) and phylogenetic implications. – Organisms Diversity & Evolution 7: 207-230.

Beutel, R.G., Yavorskaya, M.I., Mashimo, Y., Fukui, M. & Meusemann, K. 2017: The phylogeny of Hexapoda (Arthropoda) and the evolution of megadiversity. – Proceedings of the Arthropodan Embryological Society of Japan 51: 1-15.

Bolton, B. 2024: AntCat: an online catalog of the ants of the world. – <antcat.org>, retrieved on 7 January 2025.

Bonavita-cougourdan, A. & Poveda, A. 1972: Étude préliminaire d'un organe mettant en rapport intestin moyen et intestin postérieur chez les larves de fourmis (Hyménoptères Formicidae). – Comptes Rendus (Hebdomadaires) des Séances de l'Academie des Sciences. Série D. Sciences Naturelles 275: 775-778.

Boudinot, B.E., Moosdorf, O.T.D., Beutel, R.G. & Richter, A. 2021: Anatomy and evolution of the head of *Dorylus helvolus* (Formicidae: Dorylinae): patterns of sex- and caste-limited traits in the sausagefly and the driver ant. – Journal of Morphology 282: 1616-1658.

Cecilia, A., Rack, A., Douissard, P.A., Martin, T., Dos Santos Rolo, T., Vagovič, P., Hamann, E., van de Kamp, T., Riedel, A., Fiederle, M. & Baumbach, T. 2011: LPE grown LSO: Tb scintillator films for high-resolution X-ray imaging applications at synchrotron light sources. – Nuclear Instruments and Methods in Physics Research Section A: Accelerators, Spectrometers, Detectors and Associated Equipment 648: S321-S323.

Crome, W. 1957: Zur Morphologie und Anatomie der Larve von *Oryctes nasicornis* L. (Col. Dynastidae). – Deutsche Entomologische Zeitschrift 4: 228-262.

Dewitz, H. 1877: Ueber Bau und Entwickelung des Stachels der Ameisen. – Zeitschrift für Wissenschaftliche Zoologie 28: 527-556.

Douissard, P.A., Cecilia, A., Rochet, X., Chapel, X., Martin, T., van de Kamp, T., Helfen, L., Baumbach, T., Luquot, L. & Xiao, X. 2012: A versatile indirect detector design for hard X-ray microimaging. – Journal of Instrumentation 7: art. P09016.

Emery, C. 1899: Intorno alle larve di alcune formiche. – Memorie della Reale Accademia delle Scienze dell'Istituto di Bologna 5: 3-10.

Engelkes, K., Friedrich, F., Hammel, J.U. & Haas, A. 2018: A simple setup for episcopic microtomy and a digital image processing workflow to acquire high-quality volume data and 3D surface models of small vertebrates. – Zoomorphology 137: 213-228.

Fabian, B., Russell, L., Friedrich, F. & Beutel, R.G. 2015: The larval cephalic morphology of the enigmatic boreid *Caurinus dectes* (Mecoptera) and its phylogenetic significance. – Arthropod Systematics & Phylogeny 73: 385-399.

Faragó, T., Gasilov, S., Emslie, I., Zuber, M., Helfen, L., Vogelgesang, M. & Baumbach, T. 2022: Tofu: a fast, versatile and user-friendly image processing toolkit for computed tomography. – Journal of Synchrotron Radiation 29: 916-927.

Frank, D.D. & Kronauer, D.J.C. 2024: The budding neuroscience of ant social behavior. – Annual Review of Neuroscience 47: 167-185.

Fraulob, M., Wipfler, B., Hünefeld, F., Pohl, H. & Beutel, R.G. 2012: The larval abdomen of the enigmatic Nannochoristidae (Mecoptera, Insecta). – Arthropod Structure & Development 41: 187-198.

Friedrich, F. & Beutel, R.G. 2008: The thorax of *Zorotypus* (Hexapoda, Zoraptera) and a new nomenclature for the musculature of Neoptera. – Arthropod Structure & Development 37: 29-54.

Friedrich, F. & Beutel, R.G. 2010: Goodbye Halteria? The thoracic morphology of Endopterygota (Insecta) and its phylogenetic implications. – Cladistics 26: 579-612.

Friedrich, F., Schulz, J., Kubiak, M., Beckmann, F. & Wilde, F. 2015: The larval head anatomy of *Rhyacophila* (Rhyacophilidae) with discussion on mouthpart homology and the groundplan of Trichoptera. – Journal of Morphology 276: 1505-1524.

Füller, H. 1963: Vergleichende Untersuchungen über das Skelettmuskelsystem der Chilopoden. – Abhandlungen der deutschen Akademie der Wissenschaften zu Berlin (Klasse für Chemie, Geologie und Biologie) 3: 1-98.

Gauld, I. & Bolton, B. 1988: The hymenoptera. – Oxford University Press, Oxford, UK, xii + 322 pp.

Grimaldi, D. & Engel, M.S. 2005: Evolution of the insects. – Cambridge University Press, Cambridge, UK, 772 pp.

Gutmann, W.F. 1985: Urform Pneu. – Die Bedeutung des Pneu in der Biologie. – Deutsche Bauzeitung 5: 34-36.

Hart, T., Frank, D.D., Lopes, L.E., Olivos-Cisneros, L., Lacy, K.D., Trible, W., Ritger, A., Valdés-Rodríguez, S. & Kronauer, D.J.C. 2023: Sparse and stereotyped encoding implicates a core glomerulus for ant alarm behavior. – Cell 186: 3079-3094.

Hasenfuss, I. & Kristensen, N.P. 2003: Skeleton and muscles: immatures. In: Kristensen, N.P. (Ed.): Lepidoptera, moths and butterflies, Vol. 2: Morphology, physiology, and development. Handbook of zoology, Vol. IV arthropoda: insecta, part 36. – Walter de Gruyter, Berlin, pp. 133-164.

Hennig, W. 1973: Diptera (Zweiflügler). – Handbuch der Zoologie 4: 1-337.

Hinton, H.E. 1946: On the homology and nomenclature of the setae of lepidopterous larvae with some notes on the phylogeny of the Lepidoptera. – Transactions of the Royal Entomological Society of London 97: 1-37.

Hoyle, G. & Williams, M. 1980: The musculature of *Peripatus* and its innervation. – Philosophical Transactions of the Royal Society B-Biological Sciences 288: 481-510.

Jandausch, K., Pohl, H., Aspöck, U., Winterton, S. & Beutel, R.G. 2018: Morphology of the primary larva of *Mantispa aphavexelte* Aspöck & Aspöck, 1994 (Neuroptera: Mantispidae) and phylogenetic implications to the order of Neuroptera. – Arthropod Systematics & Phylogeny 76: 529-560.

Jeantet, A.Y. 1969: Recherches histophysiologiques sur la développement post-embryonnaire et le cycle annuel de *Formica rufa* (Hyménòptere). – Insectes Sociaux 16: 87-102.

Kronauer, D.J.C. 2025: Clonal raider ants. – Current Biology 35: R7-R8.

Kronauer, D.J.C., Pierce, N.E. & Keller, L. 2012: Asexual reproduction in introduced and native populations of the ant *Cerapachys biroi*. – Molecular Ecology 21: 5221-5235.

Lappano, E.R. 1958: A morphological study of larval development in polymorphic all-worker broods of the army ant *Eciton burchelli*. – Insectes Sociaux 5: 31-66.

Lösel, P.D., van de Kamp, T., Jayme, A., Ershov, A., Faragó, T., Pichler, O., Jerome, T.N., Aadepu, N., Bremer, S., Chilingaryan, S.A., Heethoff, M., Kopmann, A., Odar, J., Schmelzle, S., Zuber, M., Wittbrodt, J., Baumbach, T. & Heuveline, V. 2020: Introducing Biomedisa as an open-source online platform for biomedical image segmentation. – Nature Communications 11: art. 5577.

Mason, W.R.M. & Huber, J.T. 1993: Chapter 2, order Hymenoptera. In: Goulet, H. & Huber, J.T. (Eds.): Hymenoptera of the world. – Agriculture Canada, Ottawa, pp. 4-12.

Masuko, K. 1989: Larval hemolymph feeding in the ant *Leptanilla japonica* by use of a specialized duct organ, the "larval hemolymph tap" (Hymenoptera: Formicidae). – Behavioral Ecology and Sociobiology 24: 127-132.

Matte, A. & Leboeuf, A.C. 2024: Ruling the unruly: Innovation in ant larval feeding led to increased caste dimorphism and social complexity. – BioRxiv; doi: 10.1101/2022.12.08.519655.

Meurville, M.P. & Leboeuf, A.C. 2021: Trophallaxis: the functions and evolution of social fluid exchange in ant colonies (Hymenoptera: Formicidae). – Myrmecological News 31: 1-30.

Negroni, M.A. & Lebouef, A.C. 2023: Metabolic division of labor in social insects. – Current Opinion in Insect Science 59: art. 101085.

Nelson, J.A. 1924: Morphology of the honeybee larva. – Journal of Agricultural Research 28: 1167-1214.

Neugart, C., Schneeberg, K. & Beutel, R.G. 2009: The morphology of the larval head of Tipulidae (Diptera, Insecta) - the dipteran groundplan and evolutionary trends. – Zoologischer Anzeiger 248: 213-235.

Nitschmann, J. 1959: Die Entwicklung des Darmkanals bei *Myrmica ruginodis* Nyl. (Hym. Formicidae). – Deutsche Entomologische Zeitschrift 6: 454-463.

Ofer, J. 1970: *Polyrhachis simplex*. The weaver ant of Israel. – Insectes Sociaux 17: 49-82.

Ortius-Lechner, D., Rüger, M. & Wanke, T. 2003: Sexing at the larval stage in two ant species of the Formicoxenini (Hymenoptera). – Zoomorphology 122: 41-45.

Paganin, D., Mayo, S.C., Gureyev, T.E., Miller, P.R. & Wilkins, S.W. 2002: Simultaneous phase and amplitude extraction from a single defocused image of a homogeneous object. – Journal of Microscopy 206: 33-40.

Parker, H.L. 1935: Note on the anatomy of tenthredinid larvae with special reference to the head. – Bollettino del Laboratorio di Zoologia Generale e Agraria della R. Scuola Superiore d' Agricoltura in Portici 28: 159-191.

Penick, C.A., Ebie, J. & Moore, D. 2014: A non-destructive method for identifying the sex of ant larvae. – Insectes Sociaux 61: 51-55.

Pérez, C. 1902: Contribution a l'étude des métamorphoses. – Bulletin Scientifique de la France et de la Belgique 37: 195-427.

Peters, R.S., Meusemann, K., Petersen, M., Mayer, C., Wilbrandt, J., Ziesmann, T., Donath, A., Kjer, K.M., Aspöck, U., Aspöck, H., Aberer, A., Stamatakis, A., Friedrich, F., Hünefeld, F., Niehuis, O., Beutel, R.G. & Misof, B. 2014: The evolutionary history of holometabolous insects inferred from transcriptome-based phylogeny and comprehensive morphological data. – BioMed Central Evolutionary Biology 14: art. 52.

Petralia, R.S. & Hout, C.F. 1986: Morphology of the labial gland system of the mature larva of the black carpenter ant, *Camponotus pennsylvanicus* (DeGeer). – Proceedings of the Iowa Academy of Science 93: 16-20.

Petralia, R.S. & Vinson, S.B. 1979: Developmental morphology of larvae and eggs of the imported fire ant, *Solenopsis invicta*. – Annals of the Entomological Society of America 72: 472-484.

Petralia, R.S. & Vinson, S.B. 1980: Internal anatomy of the fourth instar larva of the imported fire ant, *Solenopsis invicta* Buren (Hymenoptera: Formicidae). – International Journal of Insect Morphology and Embryology 9: 89-106.

Piekarski, P.K., Valdés-Rodríguez, S. & Kronauer, D.J. 2023: Conditional indirect genetic effects of caregivers on brood in the clonal raider ant. – Behavioral Ecology 34: 642-652.

Pohl, H. 2010: A scanning electron microscopy specimen holder for viewing different angles of a single specimen. – Microscopy Research and Technique 73: 1073-1076.

Rafiqi, A.M., Rajakumar, A. & Abouheif, E. 2020: Origin and elaboration of a major evolutionary transition in individuality. – Nature 585: 239-244.

Rajakumar, A., Pontieri, L., Li, R., Larsen, R.S. & Vásquez-Correa, A. 2024: From egg to adult: a developmental table of the ant *Monomorium pharaonis*. – Journal of Experimental Zoology Part B: Molecular and Developmental Evolution 342: 557-585.

Richter, A., Boudinot, B.E., Yamamoto, S., Katzke, J. & Beutel, R.G. 2022: The first reconstruction of the head anatomy of a Cretaceous insect, †*Gerontoformica gracilis* (Hymenoptera: Formicidae), and the early evolution of ants. – Insect Systematics and Diversity 6(5): art. 4.

Richter, A., Garcia, F.H., Keller, R.A., Billen, J., Economo, E. & Beutel, R.G. 2020: Comparative analysis of worker head anatomy of *Formica* and *Brachyponera* (Hymenoptera: Formicidae). – Arthropod Systematics & Phylogeny 78: 133-170.

Romiguier, J., Borowiec, M.L., Weyna, A., Helleu, Q., Loire, E., La Mendola, C., Rabeling, C., Fisher, B.L., Ward, P.S. & Keller, L. 2022: Ant phylogenomics reveals a natural selection hotspot preceding the origin of complex eusociality. – Current Biology 32: 2942-2947.

Schneeberg, K., Friedrich, F., Courtney, G.W., Wipfler, B. & Beutel, R.G. 2012: The larvae of Nymphomyiidae (Diptera, Insecta) - ancestral and highly derived? – Arthropod Structure & Development 41: 293-301.

Schulman, V.K., Dobi, K.C. & Baylies, M.K. 2015: Morphogenesis of the somatic musculature in *Drosophila melanogaster*. – Wiley Interdisciplinary Reviews: Developmental Biology 4: 313-334.

Schultner, E., Oettler, J. & Helanterä, H. 2017: The role of brood in eusocial Hymenoptera. – Quarterly Review of Biology 92: 39-78.

Schultner, E., Wallner, T., Dofka, B., Brülhart, J., Heinze, J., Freitak, D., Pokorny, T. & Oettler, J. 2023: Queens control caste allocation in the ant *Cardiocondyla obscurior*. – Proceedings of the Royal Society B-Biological Sciences 290: art. 20221784.

Short, J.R.T. 1951: The morphology of the head of larval Hymenoptera with special reference to the head of the Ichneumonoidea, including a classification of the final instar larvae of the Braconidae. – Transactions of the Royal Entomological Society, London 103: 27-66.

Smith, D.R. & Middlekauff, W.W. 1987: Suborder Symphyta. In: Stehr, F.W. (Ed.): Immature insects, Vol. I. – Kendall / Hunt Publishing Company, Dubuque, IA, pp. 618-648.

Snodgrass, R.E. 1935: Principles of insect morphology. – McGraw-Hill, New York, NY, 768 pp.

Solis, D.R., Caetano, F.H., Yabuki, A.T., Moretti, T.C. & Bueno, O.C. 2009: Ultramorphology of the digestive tract of *Paratrechina longicornis* (Hymenoptera, Formicidae). – Sociobiology 53: 51-59.

Trible, W., Mckenzie, S.K. & Kronauer, D.J.C. 2020: Globally invasive populations of the clonal raider ant are derived from Bangladesh. – Biology Letter 16: art. 20200105.

Tschinkel, W.R. 2006: The fire ants. – Harvard University Press, Cambridge, MA, 723 pp.

Valentini, S. 1951: Sur l'adaptation des larves de Formicoidea. – Annales des Sciences Naturelles de Zoologie 13: 249-276.

Vilhelmsen, L. 1997: The phylogeny of lower Hymenoptera (Insecta), with a summary of the early evolutionary history of the order. – Journal of Zoological Systematics and Evolutionary Research 35: 49-70.

Vilhelmsen, L. 2003: Larval anatomy of Orussidae (Hymenoptera). – Journal of Hymenoptera Research 12: 346-354.

Villet, M.H., Hanrahan, S.A. & Walther, C. 1990: Larval structures associated with larva-to-adult trophallaxis in *Platythyrea* (Hymenoptera: Formicidae). – International Journal of Insect Morphology and Embryology 19: 243-256.

Vogelgesang, M., Farago, T., Morgeneyer, T.F., Helfen, L., Dos Santos Rolo, T., Myagotin, A. & Baumbach, T. 2016: Real-time image-content-based beamline control for smart 4D X-ray imaging. – Journal of Synchrotron Radiation 23: 1254-1263.

von Kéler, S. 1963: Entomologisches Wörterbuch. – Akademie Verlag, Berlin, 750 pp.

Weir, J.S. 1957: The functional anatomy of the mid-gut of larvae of the ant, *Myrmica*. – Quarterly Journal of Microscopical Science 98: 499-506.

Weir, J.S. 1959: Changes in the retro-cerebral endocrine system of larvae of *Myrmica*, and their relation to larval growth and development. – Insectes Sociaux 6: 27-386.

Went, F.W., Wheeler, J. & Wheeler, G.C. 1972: Feeding and digestion in some ants (*Veromessor* and *Manica*). – BioScience 22: 82-88.

Wheeler, G.C. 1928: The larva of *Leptanilla* (Hym.: Formicidae). – Psyche (Cambridge) 35: 85-91.

Wheeler, G.C. & Wheeler, J. 1957: The larva of *Simopelta* (Hymenoptera: Formicidae). – Proceedings of the Entomological Society of Washington 59: 191-194.

Wheeler, G.C. & Wheeler, J. 1961 [1960]: Techniques for the study of ant larvae. – Psyche (Cambridge) 67: 87-94.

Wheeler, G.C. & Wheeler, J. 1972: The subfamilies of Formicidae. – Proceedings of the Entomological Society of Washington 74: 35-45.

Wheeler, G.C. & Wheeler, J. 1976: Ant larvae: review and synthesis. – Memoirs of the Entomological Society of Washington 7: 1-108.

Wheeler, G.C. & Wheeler, J. 1979: Larvae of the social Hymenoptera. In: Hermann, H.R. (Ed.): Social insects. Volume 1. – Academic Press, New York, NY, pp. 287-338.

Wheeler, G.C. & Wheeler, J. 1986: Ten-year supplement to "Ant larvae: review and synthesis". – Proceedings of the Entomological Society of Washington 88: 684-702.

Wheeler, G.C., Wheeler, J. & Taylor, R.W. 1980: The larval and egg stages of the primitive ant *Nothomyrmecia macrops* Clark (Hymenoptera: Formicidae). – Journal of the Australian Entomological Society 19: 131-137.

Wheeler, W.M. 1910: Ants: their structure, development and behavior. – Columbia University Press, New York, NY, 663 pp.

Wheeler, W.M. 1918: A study of some ant larvae, with a consideration of the origin and meaning of the social habit among insects. – Proceedings of the American Philosophical Society 57: 293-343.

Wheeler, W.M. & Bailey, I. 1920: The feeding habits of Pseudomyrmines and other ants. – Transactions of the American Philosophical Society 22: 235-279.

Winston, M.L. 1991: The biology of the honey bee. – Harvard University Press, Cambridge, MA, 294 pp.

Wipfler, B., Courtney, G.W., Craig, D.A. & Beutel, R.G. 2012: First μ-CT-based 3D reconstruction of a dipteran larva – the head morphology of *Protanyderus* (Tanyderidae) and its phylogenetic implications. – Journal of Morphology 273: 968-980.

Yamada, A., Nguyen, D.D. & Eguchi, K. 2020: Unveiling the morphology of the Oriental rare monotypic ant genus *Opamyrma* Yamane, Bui & Eguchi, 2008 (Hymenoptera: Formicidae: Leptanillinae) and its evolutionary implications, with first descriptions of the male, larva, tentorium, and sting apparatus. – Myrmecological News 30: 27-52.

Yavorskaya, M., Kojima, K., Machida, R. & Beutel, R.G. 2015: Morphology of the first instar larva of *Tenomerga mucida* (Chevrolat, 1829) (Coleoptera: Archostemata: Cupedidae). – Arthropod Systematics & Phylogeny 73: 239-258.

Yoder, M.J., Mikó, I., Seltmann, K.C., Bertone, M.A. & Deans, A.R. 2010: A gross anatomy ontology for Hymenoptera. – Public Library of Science One 5: art. e15991.

Yuasa, H. 1922: A classification of the larvae of the Tenthredinoidea. – Ph.D. thesis, University of Illinois Press, Champaign, IL, 263 pp.

Zara, F.J. & Caetano, F.H. 2002: Ultrastructure of the salivary glands of *Pachycondyla* (= *Neoponera*) *villosa* (Fabricius) (Formicidae: Ponerinae): functional changes during the last larval instar. – Cytologia 67: 267-280.

Zara, F.J. & Caetano, F.H. 2004: Ultramorphology and histochemistry of fat body cells from last instar larval of the *Pachycondyla* (= *Neoponera*) *villosa* (Fabricius) (Formicidae: Ponerinae). – Brazilian Journal of Biology 64: 725-735.

Zimmermann, D. & Vilhelmsen, L. 2016: The sister group of Aculeata (Hymenoptera) - evidence from internal head anatomy, with emphasis on the tentorium. – Arthropod Systematics & Phylogeny 74: 195-218.